LUT UNIVERSITY

LUT School of Energy Systems

LUT Mechanical Engineering

Timo Koistila

FLOW ACCELERATED CORROSION IN NUCLEAR POWER PLANT SECONDARY CIRCUIT

2021

TIIVISTELMÄ

Timo Koistila

Virtauksen kiihdyttämä korroosio ydinvoimalaitoksen sekundääri piirissä

Diplomityö

2021

88 sivua, 27 kuvaa, 10 taulukkoa ja 5 liitettä

Useissa ydinvoimalaitoksissa ja muissa prosessiteollisuuden laitoksissa on kohdattu vakaviakin ongelmia virtauksen edistämän korroosion johdosta. Nykyään tämä ongelma on paremmin otettu huomioon ja ymmärretään kuinka sen aiheuttamat ongelmat voidaan minimoida, tai ainakin ottaa huomioon vuositarkastuksia suunnitellessä. Ongelmana tässä on, että kaikkia putkia tai muita kohteita ei voida tarkistaa. Tarvitaan siis jokin työkalu, jolla seuranta voidaan kohtistaa tarkemmin niille alueille, joissa virtauksen edistämää korroosiota todennäköisimmin esiintyy.

Ennen kuin tätä voidaan lähteä ennustamaa, tulee ymmärtää mistä korroosio johtuu ja mitkä asiat vaikuttavat sen suuruuteen. Esimerkiksi pH:n vaikutus korroosioon on merkittävä. Muita tärkeitä parametrejä ovat lämpötila, sillä kun lämpötila on tarpeeksi alhainen, korroosiota ei esiinny merkittävästi. Korroosion nopeus kasvaa aina lämpötilaan 150-180 °C, jonka jälkeen se taas pienenee. Materiaalit ja erityisesti Kromin pitoisuus metallissa taas parantaa kestävyyttä. Yhtä iso vaikutus on itse putkiston reitityksellä. Kaikki virtausvastukset aiheuttavat pyörteisyyttä ja näin ollen lisäävät korroosiota.

Näistä lähtökohdista aloimme rakentamaan omaa laskentamallia virtauksen edistämälle korroosiolle. Vesille käytimme mallia, jonka pohjana toimii aineensiirtokerroin ja vesi-höyry seoksille mallia, jossa käytetään kertoimia suoraan kirjallisuudesta. Useat kaupalliset laskentaohjelmat käyttävät samoja parametrejä, mutta se mikä meiltä puuttuu, on data tutkimuslaitoksilta. Kaupalliset ohjelmat käyttävätkin paljon erilaisia kertoimia laskuissaan, jotta tulokset olisivat vastaavia kuin jo mitatuissa tutkimuksissa. Tiedostimme asian ja tarkoituksena olikin kehittää malli, jolla pääsisimme vertailemaan tuloksia omien laskujen kautta, ei niinkään yksittäistä tulosta. Molemmilla malleilla saamme arvioitua korroosion suuruuden, mutta vedelle tulokset ovat selvästi pienempiä kuin referenssi laskuissa. Vastaavasti vesi-höyry kaavoilla saamme hieman suurempia arvoja kuin vertailulaskuissa.

ABSTRACT

LUT University
LUT School of Energy Systems
LUT Mechanical Engineering

Timo Koistila

Flow accelerated corrosion in nuclear power plant secondary circuit

Master's thesis

2021

88 pages, 27 figures, 10 tables and 5 appendices

Examiners: Professor Harri Eskelinen
            PhD. Mladenka Lukaycheva

Keywords: Flow accelerated corrosion, Corrosion,

Several nuclear power plants and in process industry in general have faced severe problems with the flow accelerated corrosion. Today the issue is better taken into account and the problems can be minimized or at least taken into account when planning yearly inspection plan. Problem with the inspection plan is that not all the pipes can be inspected. This has created the need for program that could pinpoint the locations where the flow accelerated corrosion most probably occur.

Before you can predict the corrosion rate, you should understand what causes corrosion and what parameters affect the severity of it. For example, the pH impact on corrosion is significant. Other key parameters are temperature, since when the temperature is low, or high enough the corrosion rate decreases. The rate is at the highest when the temperature is between 150 to 180 °C. Materials, especially the Chromium content in metal improve the resistance to the corrosion. As big of an impact to the corrosion rate is the actual pipe routing.

From this standpoint we started building our own calculation model. For the one-phase flow calculation we used a model that is based on mass transfer coefficient and for the two-phase flow calculation we used coefficients to estimate the corrosion rates. Many of the commercially available calculation programs use the same parameters but what we are lacking is the data from the research and from the real measured corrosion rates form existing plants. The existing software's use different kind of coefficient in their calculation to get the same values as in the existing plants. We acknowledge this and the purpose was to develop a model to compare the results and to define the locations where the flow accelerated corrosion might be most severe. With both models we are able to get results for the corrosion rates, but the one-phase flow results seem to be a lot smaller than the ones in the reference calculation. On the other hand, the two-phase flow calculation seems to give a bit too high corrosion rates compare to the reference calculation. We assume this to be from the missing coefficient they have used since the initial data is the same.

ACKNOWLEDGEMENTS

It has been a long road until this point but finally the graduation is at sight. There are many people who has helped me on the way but first I would like to thank our study group here at Helsinki for organizing regular study session. That helped a lot and brought some regularity to my otherwise unregular studying.

I want also to thank my examiners Harri and Mladenka for helping with the Thesis and pushing me forward when we hit obstacles on the way. And trust me, there were some…

Finally, I own biggest thank you to my family. You have given me time when I have needed it and supported me on the way. Tiia, I promise I will make this up for you.

1.12.2021

Timo Koistila

TABLE OF CONTENTS

Appendix I: Numerical values for points 1 & 2.

Appendix II: Numerical values for points 3 & pH.

Appendix III: Numerical values for temperature & 4.

Appendix IV: Numerical values for points 5 & 6.

Appendix V: Numerical values for steam fractions

LIST OF SYMBOLS AND ABBREVIATIONS

Symbols

A	Cross-section area	[m^2]
CP	Corrosion Penetration	
CR	Corrosion Rate	
C_s	Fe^{2+} concentration at the surface of water-oxide inferace	[μg/kg]
C_∞	Fe^{2+} concentration in the flow	[μg/kg]
d	diameter	
D	Diffusivity of Fe ions	[m^2/s]
E	Electrochemical Potential	[V]
f(t)	Temperature correlation factor	
f(x)	Moisture correlation factor	
pH	Hydrogen potential	
k	mass transfer coefficient	[m/s]
k_c	Keller coefficient	
ṁ	Mass flow	[kg/s]
mm	millimeter	
n	nano	[10^{-9}]
p	density	[kg/m^3]
Re	Reynold's number	
Sh	Sherwood number	
Sc	Schmidt number	
V	Flow speed	[m/s]
v	Kinematic viscosity	[m^2/s]
wt%	Weight percentage	

Abbreviations

atm   atmospheric

FAC   Flow Accelerated Corrosion

MSR   Moisture Separator Re-heater

NPP   Nuclear Power Plant

SHE   Standard Hydrogen Electrode

VVER   Vodo-Vodyanoi Energetichesky Reaktor (Water-Water Energetic Reactor)

1   INTRODUCTION

There has been several severe flow accelerated corrosion incident's in nuclear power plants secondary circuit that has caused a production losses, or in worst case, casualties. Typically, these problems occur suddenly and without warning. Therefore, the nuclear power plans have prepared the inspection plan for the power units. Purpose of the plan is to focus the inspections on the locations where the possible wall thinning might occur. The problem is how to define these locations?

1.1   Research background

The need for this thesis came from when we started thinking of our nuclear power plant operating life expectancy. Are there something we haven't checked or if some issues should be double checked? The most critical components are designed to last for 60 years of operation, but these are typically located in containment building and in the primary circuit. In other words, in a location where replacement is very time consuming and costly. Then we expanded our view a bit more and started thinking about components and pipes in secondary circuit. There the replacement is a lot easier because they are not nuclear safety classified and the lay-out has been designed so that the maintenance is easier.

The planned operating years was perhaps the first idea of the thesis but soon after the first discussions, we started focusing on the maintenance and inspection plans for the unit. Idea of course is to have such a good inspection program that there are only preventive and scheduled maintenance done during operation, refueling and maintenance breaks. But since the time to do the maintenance and the inspections is limited, not all the location can be inspected as frequently. So, there should be a method of estimating what are the critical location that are inspected on a more frequent basis.

The unplanned maintenance is expensive if you need to limit the unit operating hours or the load because of a sudden failure. Other aspect to the sudden failures is safety. In case of secondary circuit, we are typically not talking about nuclear safety but personnel safety. There are several incidents reported around the word on nuclear power plant about the

corrosion problems that has resulted in personnel injury or even death. Couple of examples are given in chapter 2.

1.2   Master thesis targets

This thesis has three main targets. First target is to highlight the importance of Flow Accelerated Corrosion to nuclear power plants. In this case especially to VVER type of plants. This topic is discussed in several chapters from different angles. In some chapters we discuss about the unplanned maintenance cost and production losses, in some chapters we discuss about the personnel safety and in some parts, we discuss about the inspection programs to avoid these kinds of problems. First, we discuss about corrosion in general and then we focus on a FAC. In chapter 3 it is explained why the FAC can be a problem that evolve hidden, and the first warning is the pipe rupture.

The second target is to define the locations of VVER type plant, where is the highest probability for FAC development. We define the key parameters affecting the FAC speed and ways to prevent or minimize the excess pipe thinning. If the operators can define the location that are most prone for FAC, they can develop the inspection programs so that these areas are measured more frequently. In case of a new build plant, it's even possible to solve the problem by design solutions.

The third and the most important one is to develop a calculation model for estimating the corrosion rate on a given location and parameters. With this kind of tool, it is possible to estimate the operation years for a pipe or to estimate what kind of changes is needed for the process parameters to reach the needed operation years.

1.3   Research problem

The research problem defined for this thesis is, what are the most influencing parameters affecting flow accelerated corrosion and how to define the locations where it might occur. It is possible to name several factors that are known to have impact on corrosion rate but what is the actual impact of those individual factors? Is it possible to create a calculation tool to estimate the corrosion rate, not only with fixed process parameters but also with variable ones?

1.4   Research methods

All starts from the basics of corrosion. What are the parameters affecting on it and is there a way to estimate how prone to corrosion some metals are? When the basics are covered the focus is on the flow accelerated corrosion. In chapter 3 the parameters influencing FAC rate is explained. Based on these parameters, the calculation tool for the corrosion rate is created. The tool is created for both single- and two-phase flows. Both have same affecting parameters, but the two-phase flow has the moisture content factor included into the calculations.

The single-phase flow calculation tool is based on the mass transfer coefficient form the surface of the metal and from the protective oxide layer. This coefficient is the basis for the calculation and is a function of several parameters affecting the corrosion rate. The two-phase flow calculations are based on the coefficients for different process parameters directly. More detailed information about the calculation methods is given in Chapter 4 and how the tools are used for the calculations is described in Chapter 5.

1.5   Limitations

In the Thesis we focus only on wet corrosion that is the form of the corrosion in nuclear power plants as in the process industry in general. The wet or electrochemical corrosion have several different forms such as crevice corrosion or stress corrosion cracking. These are explained in the Chapter 2 but are not considered the equations.

The erosion corrosion is left out from the equations even though it is often used as synonym for the FAC. They are two different things, but both are caused by the flow. Erosion is based on the mechanical degrading of the wall due to impacts from particles or water droplets. Erosion can also occur if the flow speed is too high that will cause the shear stress on an oxide layer to increase and peel off the layer. In this sense the erosion corrosion is a function of a flow but not considered as a wet corrosion form but as a mechanical one.

1.6   Expected contribution

The expectation is to create a calculation tool that can be used to estimate corrosion rates and to define the locations where the most severe corrosion rates occur. The tool shall be

used to estimate corrosion rate on a different location having different process parameters. The results shall be used as an input for the inspections plans created for the unit.

The importance of the flow accelerated corrosion is to be highlighted so the possible problems occurring are well known in advance and that the mitigation of these problems is done to the extent possible. The FAC should be taken into consideration well in the design phase and to be implemented into the inspection and maintenance plant of the operating plant.

2   CORROSION PHENOMENA

Generally, corrosion is degradation of metals through reactions with the environment. Corrosion can occur through two type of reactions: chemical (dry corrosion) and electrochemical (wet corrosion). Which of them will take place depend on environmental conditions. Chemical corrosion is mostly common for high temperatures and dry media (nonconductive environment). In opposite, electrochemical corrosion require conductive environment. Depending on damages form, there are again two types of corrosion – uniform and local (see chapter 2.2). A common misconception is that only iron corrodes since this is easily visibly to naked eyes as a rust. Rust is oxidized iron and therefore it's a result of corrosion with red or brown flakes on an iron surface. But also other metals corrode, for example copper corrodes and produce a protective green layer on the metal surface. (McCafferty 2010, p. 13.)

Chemical corrosion does not occur so often and require more specific conditions, that is why it will not be discussed here. Electrochemical corrosion of metals and alloys usually happens as an electrochemical reaction in ionically conducting medium (electrolyte). In fact, this electrochemical reaction is an oxidation-reduction reaction, which can be divided in two semi-reactions: oxidation and reduction, happening in the same or different places. Electrochemical reaction requires four elements: an anode, a cathode, a metallic conductor, and an electrolyte.

The possibility for metal to corrode and rate of corrosion depend on metal itself and characteristics of environment, as a general estimation for metal behavior can be made based on its Electrochemical potential.

Electrochemical electrode potential is result of appearance of polarity on the borderline between metal (electronic conductor) and electrolyte (ionic conductor). When the metal is in contact with environment containing same metal ions and only these ions take place in electrochemical reaction, the potential is called Equilibrium electrode potential.

When Equilibrium electrode potential is measured by Standard electrode at standard conditions it is called Standard Electrode potential. Table 2.1 presents extract from table of

standard electrode potentials for given reactions measured toward the Standard Hydrogen Electrode (SHE). The value of hydrogen electrode potential is accepted to be 0 V at standard conditions (1atm, 20 °C and concentration 1 mol/l). Potentials are all referred to the reduction reactions (the cathode half reactions). Typically, term nobility is used to describe position in the table. Metals with positive potentials have higher nobility than the negative ones. Higher the nobility, less likely they will corrode/react with environment.

Table 2.1 Standard electrode potential series (SHE) (Pedeferri 2018, p. 42-43.)

Electrode reactions	E V (SHE)	Electrode reactions	E V (SHE)
$O_3 + 2H^+ + e^- \rightarrow O_2 + H_2O$	2,07	$Sn^{4+} + 2e^- \rightarrow Sn^{2+}$	0,15
$Co^{3+} + 3e^- \rightarrow Co$	1,842	$2H^+ + 2e^- \rightarrow H_2$	0
$Au^+ + e^- \rightarrow Au$	1,68	$2D^+ + 2e^- \rightarrow D_2$	-0,003
$Mn^{3+} + e^- \rightarrow Mn^{2+}$	1,51	$Fe^{3+} + 3e^- \rightarrow Fe$	-0,036
$Cl_2 + 2e^- \rightarrow 2Cl^-$	1,358	$Mo^{3+} + 3e^- \rightarrow Mo$	-0,2
$O_2 + 4H^+ + 4e^- \rightarrow 2H_2O$	1,23	$Co^{2+} + 2e^- \rightarrow Co$	-0,28
$HNO_3 + 3H^+ + 3e^- \rightarrow NO + 2H_2O$	0,96	$Cr^{3+} + e^- \rightarrow Cr^{2+}$	-0,41
$2Hg^{2+} + 2e^- \rightarrow Hg_2^{2+}$	0,92	$Fe^{2+} + 2e^- \rightarrow Fe$	-0,44
$Hg^{2+} + 2e^- \rightarrow 2Hg$	0,851	$Cr^{3+} + 3e^- \rightarrow Cr$	-0,74
$Fe^{3+} + e^- \rightarrow Fe^{2+}$	0,77	$Cr^{2+} + 2e^- \rightarrow Cr$	-0,913
$O_2 + 2H^+ + 2e^- \rightarrow H_2O$	0,682	$Nb^{3+} + 3e^- \rightarrow Nb$	-1,1
$2NO^{3-} + 6H_2O + 10e^- \rightarrow N2 + 12OH^-$	0,25	$Na^+ + e^- \rightarrow Na$	-2,71
$AgCl + e^- \rightarrow Ag + Cl^-$	0,22	$Ca^{2+} + 2e^- \rightarrow Ca$	-2,86
$SO_4^{2-} + 2e^- + 2H^+ \rightarrow SO_3^{2-} + H_2O$	0,17	$Li^+ + e^- \rightarrow Li$	-3,05

In reality, metals and alloys are in contact with variety of environments containing a lot of other species which also can take place in electrochemical reaction. Then, we do not speak for Standard electrode potential any longer, but for Corrosion potential.

Corrosion potential can be measured by different reference electrodes immersed also in the environment and connected with the metal through voltmeter. Voltmeter measures the difference between both electrodes' potentials, which is called Electromotive force. In industry, corrosion potentials measured in this way for different metals and alloys in the same environment are used for material selection. Such kind of corrosion potentials series are called Galvanic series In practice, Galvanic series are used as a bases for proper material selection, which is one of the most important measures for mitigate corrosion, also in case of FAC.

Unfortunately, except difference in two metal electrodes potentials, usually there are differences in potential at specific areas on the same metal surface. This is the reason for corrosion to start. These differences can appear because of inhomogeneity in the metal itself or because inhomogeneity in environment. Whatever the inhomogeneity is, more positive and more negative sites form on the metal surface. These areas are called anodes (more negative) and cathodes (more positive) and form galvanic cells on the surface.

$$\Delta E = E_c - E_a \tag{2.1}$$

Rate of corrosion depends on the difference between anode (E_a) and cathode (E_c) potentials, which can be expressed by Electromotive force (ΔE).

Electrochemical corrosion reaction can be presented by work of galvanic cells. Metal ion leaves the metal surface at the anode and goes into solution. Electrons stays in the metal and move in cathodes direction; therefore, metal is oxidized at the anode. This is called anodic reaction.

$$2Fe_{(s)} \rightarrow 2Fe^{2+}_{(aqueous\ solution)} + 4e^- \tag{2.2}$$

One of possible anodic reactions for iron is shown in equation 2.2. Cathodic reaction occurs on a cathode where different species, as example positively charged ions from electrolyte consume released electrons transferred through the metal.

$$O_{2(gas)} + 2H_2O + 4e^- \rightarrow 4OH^-_{(aqueous)} \tag{2.3}$$

$$2H^+ + 2e^- \rightarrow H_2\uparrow \tag{2.4}$$
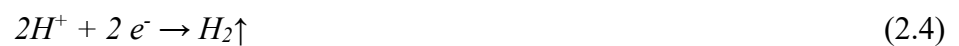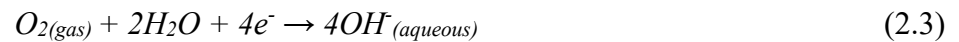
Typical cathodic reaction is a reduction of dissolved oxygen forming hydroxide ions shown in equation 2.3 or reduction of hydrogen ions to hydrogen gas in 2.4. Other ions and molecules presented in the environment, even dissolved ions of the metal itself, also can be reduced on the cathode places. (Papavinasam 2014, p. 249-256)

Corrosion takes place only if both, anode and cathode reactions take place simultaneously, there's an electrolytic conductor and a metallic conductor. The anodes, cathodes and metallic conductors are already in the base metal itself and those cannot be excluded when planning corrosion control strategies. Figure 2.1 shows how the corrosion reaction happens simultaneously on metal and electrolytic conductor. Metal is oxidized at the anode by releasing Fe^{2+} ions into the solution. Electrons are transferred via metallic path to cathode where they are reacting with ions in the solution. The electronic current flows from cathode to the anode, opposite of the electron flow.
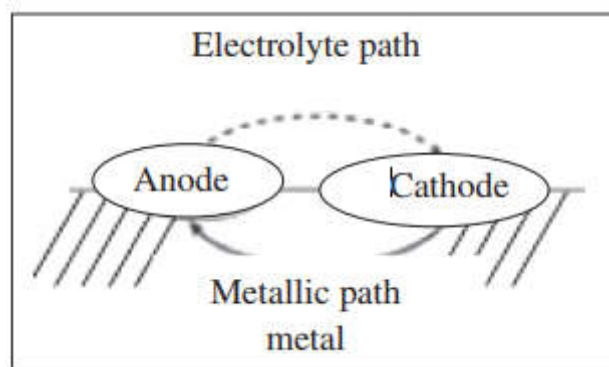
Figure 2.1. Example how the anode, cathode and electrolytic conductor are connected. (Papavinasam 2014, p. 256.)

As shortly mentioned above, reason why both anode and cathode can be present in the metal lies in the heterogeneous nature of the metal surface. No matter how well the casting and forming of metal is done, there're always different kind of grains and grain boundaries in the metal surface. There're always some impurities or it can adsorb ions from the solution that changes the surface energy of the metal atoms around it. Atoms at the highest energy sites are the ones that get passed into solution in form of ions. Typically, these high energy sites are located on edges, or on defects. Strained or stressed areas are also high energy sites where the corrosion typically start since they tend to give up atoms more easily than the atoms in the unstrained regions. When the metal dissolution process starts, a new high energy sites are created and the position of the cathode and anode change randomly eventually creating a

uniform corrosion rate on a base metal. (Papavinasam 2014, p. 249-256.)

2.1 Corrosion rate expression

Corrosion rate CR can be expressed in different units. Typically, it is expressed by mass loss per unit area per time.

$$CR = \frac{\Delta m}{A * t} \qquad (2.5)$$

Where Δm is the difference of the mass before and after corrosion, A is the area and t is time and CR is the mass loss as expressed in equation 2.5. As an example, units can be kg/m² year, or mg/m²h.

As example: $\frac{kg}{m^2 yr}$ (kilograms per meter squire per year), or $\frac{gr}{m^2 day}$ (grams per meter squire per day), etc.

Corrosion penetration (CP) – mm/y (millimeter per year)

This will give directly the material loss or the thickness loss in given time, typically in a year. Conversion equation is shown in equation 2.6 where the CR stands for corrosion rate, expressed in equation 2.5 and ρ is the density.

$$\frac{mm}{year} = \frac{\Delta m}{A * t * \rho} = \frac{CR}{\rho} \qquad (2.6)$$

In most cases the time is set to a year to get a meaningful value for corrosion rate. This way it's easier to estimate how long for example a pipe will last with the given corrosion rate but other time intervals can be used if seemed meaningful.

It's clear from the units that the $\frac{mm}{yr}$ value gives the actual thickness loss of the given sample but the $\frac{kg}{m^2 yr}$ will give the actual material loss of a sample. If you know the gross area of the measured metal, it's possible to convert the $\frac{kg}{m^2 yr}$ to $\frac{mm}{yr}$ and vice versa. For conversion you need to know sample area A in m² and the density ρ in $\frac{kg}{m^3}$. In table 2.2 the relationship among commonly used units is presented.

Table 2.2 Conversion relationship for corrosion rate units. (McCafferty 2010, p. 24.)

	mm / year	g / m² day

mm / year	1	2,74 * ρ
g / m² day	0,365 / ρ	1

2.2 Passivation and passivity

Corrosion resistance properties of the metal could be greatly influenced by the surface conditions or by formation of the protective oxide layers. The protective layer can form either by precipitation of insoluble corrosion product or as a result of anodic reaction. First method is not typical for power plant environment but can be observed on a copper or a bronze metal when exposed to atmosphere. Second, the anodic reaction is common in process industry because it affects metals such as iron (Fe), chrome (Cr), molybdenum (Mo), tungsten (W), titanium (Ti), Zirconium (Zr) and alloys such as stainless steels.

Oxide-type layer is typically 3-5 nm thick and it has semi-conductive properties. This oxide layer protects the base metal from environment and reduce the corrosion rate and in some cases even halts the corrosion process as witnessed with stainless steel pipes. (Pedeferri 2018, p. 92-94.)

2.3 Types of corrosion

Depending on damages, corrosion can be divided into two main categories, uniform and localized corrosion. Uniform corrosion can be expressed as a general corrosion, and it affect the whole surface of the metal evenly as shown in Figure 2.2. In uniform corrosion localized anodes and cathodes change all around metal, eventually thinning metal uniformly. Typically, uniform corrosion can be found in iron structures in harsh environment such as close to seashore or on a process pipes with a steady flow.

Uniform corrosion

Galvanic corrosion

Pitting corrosion

Crevice corrosion

Intergranular corrosion

Environmental assisted cracking

Flow affected corrosion

Hydrogen damage
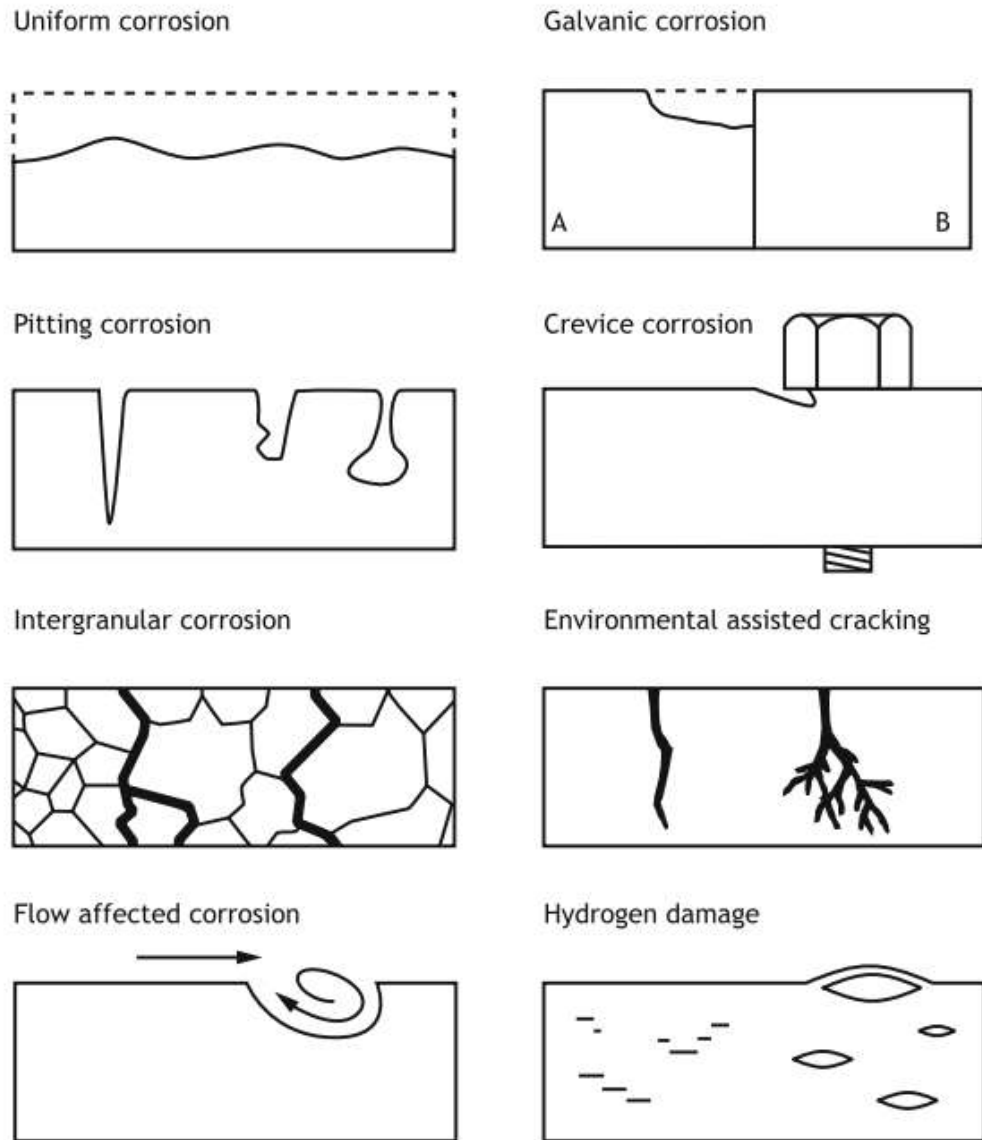
Figure 2.2 Schematic representation of different corrosion forms. (Pedeferri 2018, p. 6.)

In localized corrosion anodes and cathodes are fixed that enables material loss in a specific location. The localized corrosion can be divided in many different corrosion forms. There is no one common list of localized corrosion forms. Many different classifications of local forms of corrosion exist according different authors and based on different criteria.

One of the most commonly distinguished localized corrosion forms are:

- Crevice corrosion
- Pitting
- Stress-corrosion cracking

- Galvanic corrosion

- Intergranular corrosion

- Selective leaching

- Erosion corrosion

From these seven local forms the most common ones are Pitting, crevice and stress-corrosion cracking. (McCafferty 2010, p. 16-27.)

However, often in practice it is not possible to separate one local form from other, because as example, corrosion process can start by pitting formation on grain boundaries and continue as intergranular corrosion. Where is the place of flow accelerated corrosion and whether it have to be assigned to general or local forms of corrosion? It will be discussed in chapter 3.

In uniform corrosion form, the metal surface corrodes evenly with a steady speed and is typical for unprotected metal surfaces. The metal corrodes evenly because the anodes and cathodes change location constantly and eventually cause surface to corrode uniformly. Typically, uniform corrosion can be witnessed in metals that are located outside or in a metals exposed to chemicals. Propagation of uniform corrosion is easy to predict and to measure since it is uniform and proceeds with a steady pace. Only exception is flow accelerated corrosion that could be also classified as a form of a uniform corrosion but typically it is affecting metal in a certain location, such as elbows or orifices in a pipe.

Crevice corrosion is a localized corrosion form that starts from a sub-millimetric gab or deposit on a metal surface, under a gasket or a bolt head, or between overlapping metal sheets. Crevice corrosion can proceed in active passive alloys such as stainless steels, nickel alloys and titanium. This form of corrosion can become critical especially in heat exchangers. For example, spaces between plates, tubesheet and tube, tube and diaphragm, welding defects, supports, spacers or under deposits are great locations to let crevice corrosion to start. This can be even intensified by high heat flux or by formation of deposits or concentration of aggressive species on a boiler tube-sheet. An example could be stainless steel in contact with water solution containing Cl^- -ions.

Crevice corrosion start by incubation (oxygen depletion) stage. Oxygen inside the gab is consumed by the corrosion reactions on a passive stainless steel. Second stage start when oxygen is depleted in the crevice. Lack of oxygen in the crevice brings stainless steel into active conditions where metal ions concentrate inside the crevice and the hydrolysis begins. This cause pH value to drop as low as pH2. Because of the H^+ ions and accumulation of metallic cations in the crevice causes Cl^- ions to migrate from the bulk electrolyte to maintain charge neutrality within the crevice solution as seen schematic figure 2.3.

Crevice former

Cl^-

Solution

Iron

Cl^- Fe^{+2} H^+ Fe^{+2} Cl^- H^+

Fe

Fe

$$Fe^{+2} + 2\,H_2O \longrightarrow FeO\,H^+ + H^+$$

$$\text{or, } Fe^{+2} + 2\,H_2O \longrightarrow Fe(O\,H)_2 + 2\,H^+$$
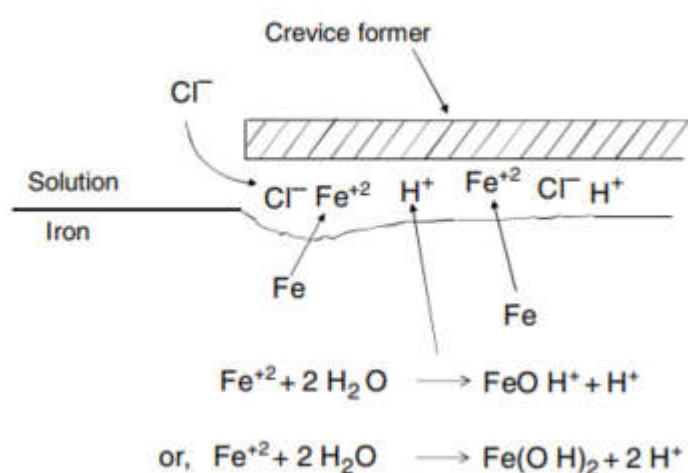
Figure 2.3 Propagation stage of crevice corrosion

Depending on a gab size, the first stage can take months or years before entering propagation stage which can proceed fast due to highly corrosive environment in the crevice. (McCafferty 2010, p. 263-272.)

Pitting corrosion is a localized corrosion form that propagates in a small area of the metal surface. Pitting corrosion starts by breaking down the protective passive film by aggressive anions, typically chloride ions. Passive film can be broken by solid particles or by flow disturbances that creates great enough shear stress than can remove the protective layer and exposing the base metal. When the oxide film is punctured the pitting corrosion propagate same way as the crevice corrosion. The dissolved metal cations are confined in the pit resulting into hydrolysis same way as in crevice corrosion. In both of these corrosion forms, the local conditions are developed so that they are capable of sustaining further pit growth. (McCafferty 2010, p. 263-290.)

Stress corrosion cracking is initiated similar way as pitting or crevice corrosion. First the protective oxide layer is removed either by chlorides or by mechanical impact. Then the base metal starts to corrode as in the pitting corrosion. Difference to pitting- or crevice corrosion is that there is a stress applied into the base metal. This can be caused by internal or external stress. Internal stress can be present from cold forming, machining, cutting, welding or heat treatment. In other words, from residual stress in the base metal after the manufacturing. External forces are, as the name implies, from external sources such as static stress, pressure, heat expansion or vibration from equipment and process. External stresses are easier to anticipate and therefore easier to prevent than the internal ones. Both, the internal and external stress can be present at the same time enforcing the crack growth. (McCafferty 2010, p. 207-272.)

When the corrosion starts to propagate on a base metal defect, such as welding defects or mechanical grooves, the applied stress is intensified on a crack tip. At first the crack grows on a steady phase. This can be estimated when the applied stress and corroding environment is known. Eventually the crack size reaches the limit when the applied stress causes sudden break on a metal. (McCafferty 2010, p. 207-272.)

This kind of failures appear without plastic deformation. This is typical for brittle materials, but stress corrosion cracking is found on materials that are ductile, also. This is possible because the crack can propagate steadily on a grain boundary or even through the grains. Therefore, the crack propagation phase looks like a brittle crack, but the eventual failure caused by stress can be brittle or ductile. (McCafferty 2010, p. 207-272.)

Stress corrosion cracking can be prevented by selection of right materials for the environment and by limiting the applied stress and the defect size where the crack growth could start. Especially the last one is important because even if the metal is stressed below the yield strength limit, the defect causes the applied stress to intensify on a tip of the crack. (McCafferty 2010, p. 207-272.)

Erosion corrosion occurs when there is combine action of electrochemical corrosion process and mechanical impact of corrosion media itself, as example hard particles in the flow. In

this sense, FAC can be considered as a kind of erosion corrosion, when there is no direct mechanical impact of the flow, but the electrochemical reaction is accelerated by the high flow speed. The erosion-corrosion propagation speed is dependent on the erosive properties of the flow. This is caused by continuous local damage to the protective oxide film exposing the base metal. This continuous local damage can result from several factors such as turbulence, cavitation or particles in the flow. The turbulence can be so strong that it peels off the oxide layer. The cavitation is implosion of gas bubbles and this implosion create shock wases so strong it will peel off the protective oxide layer. Typically, these kind of problems can be found suction piping of pump that pumps saturated water. Particles in the flow will cause same kind of erosion-corrosion damages but on a different location. Typically, particles caused erosion-corrosion thinning can be found on elbows or in T-piecies. (Pedeferri 2018, p. 314-321.)

2.4   Corrosion problems in Nuclear Power Plant secondary circuit

On figure 2.4 the impact of FAC during different operation stages is presented. About 30 % of documented events are registered during normal operation and about 40 % of them were reasons for unplanned outages.
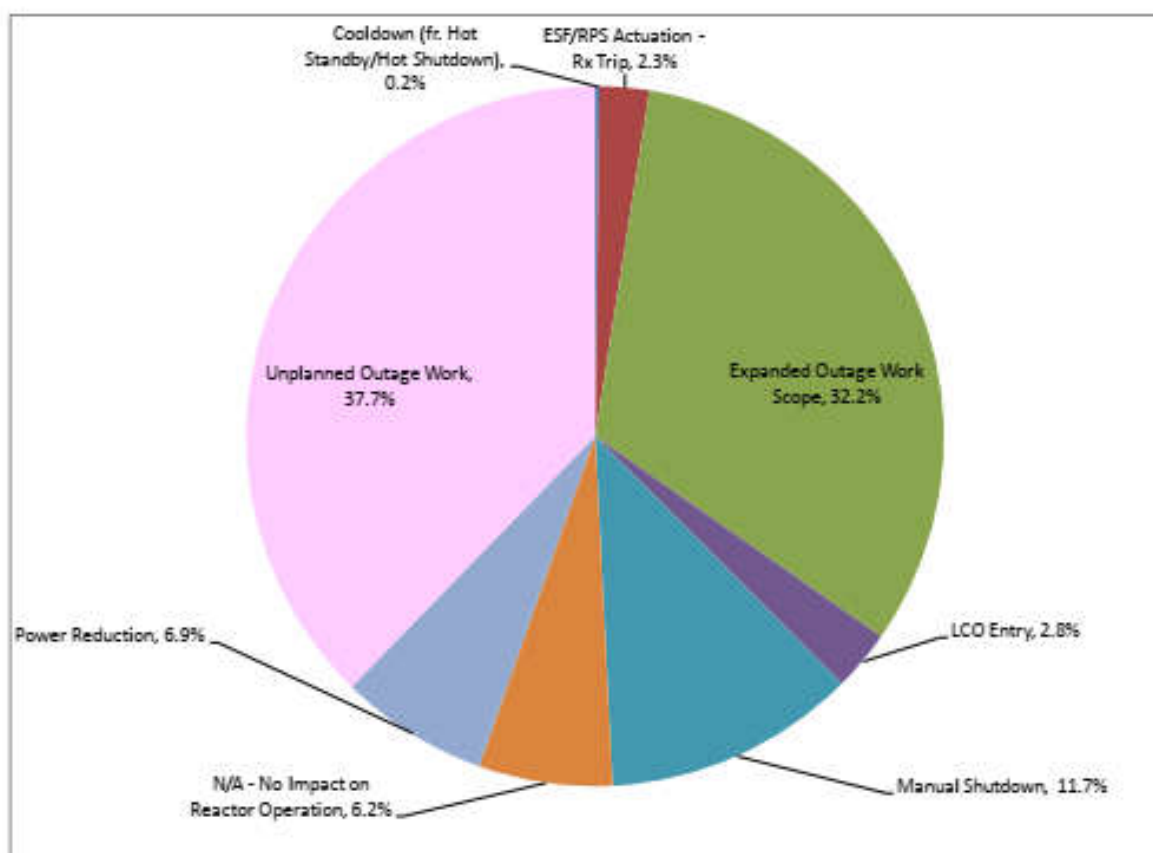
Figure 2.4 FAC Event impact on Plant operation (NEA/CSNI/R(2014)6. 2015. p.56.)

Over the years there has been several severe accidents on NPP's that are related to flow accelerated corrosion. These accidents have caused casualties and production losses to practically all the reactor types used. This chapter gives examples what could happen even on a newly build power plant if flow accelerated corrosion has not been taken into account. (NEA/CSNI/R(2014)6. 2015. p. 45-56.)

Surry 2 incident in 1986. An elbow on a main feed water pump ruptured after the reactor trip. Around 113 m³ of 190 °C feed water was released burning 8 workers, 4 of them subsequently died. Escaping steam and water also caused equipment damage and electrical malfunctions to other system. Rupture initiated at the inlet to on 90-degree elbow which was located immediately after a T-piece. Original nominal wall thickness was 12,7 mm which was reduced throughout the elbow to average of 3 mm and close to the rupture area the wall thickness was just 1.2 mm. Utility investigation concluded that the cause of wall thinning was single-phase flow accelerated corrosion. High local turbulence levels caused by the

piping geometry accelerated the process. Piping steel contained only 0,02 % chromium. (WANO report EAR ATL 90-017.)

Mihama 3 incident in 2004. Condensate pipe after low pressure pre-heaters and before deaerator ruptured while on full power. Opening was downstream an orifice plate on top of the pipe as seen in figure 2.5. Through the opening total of 885 tons of hot water and steam was released into the turbine hall where at the moment of accident were 104 persons working. Number of workers in the turbine hall was so big because they were conducting preparatory works for the upcoming inspection/maintenance outage in 5 days. From these 104 persons 11 was injured and 5 of them was killed. Investigation showed that upstream the orifice there were no substantial wall thinning. Opening was 1,25 times the pipe diameter after the orifice and the measured wall thickness at the opening was 0,4 mm when the nominal thickness was 10 mm. Interior of the pipe showed fish-scale like pattern which are typical for flow accelerated corrosion wall thinning. Investigation showed also that the second condensate line with similar geometry had suffer significant wall thinning being only 1,8 mm at 1,25 D from the orifice. It was also noted that the wall thinning became gradually mild as the distance from the orifice increased and that there was no thinning on bottom part of the pipe. Pipe material was carbon steel.
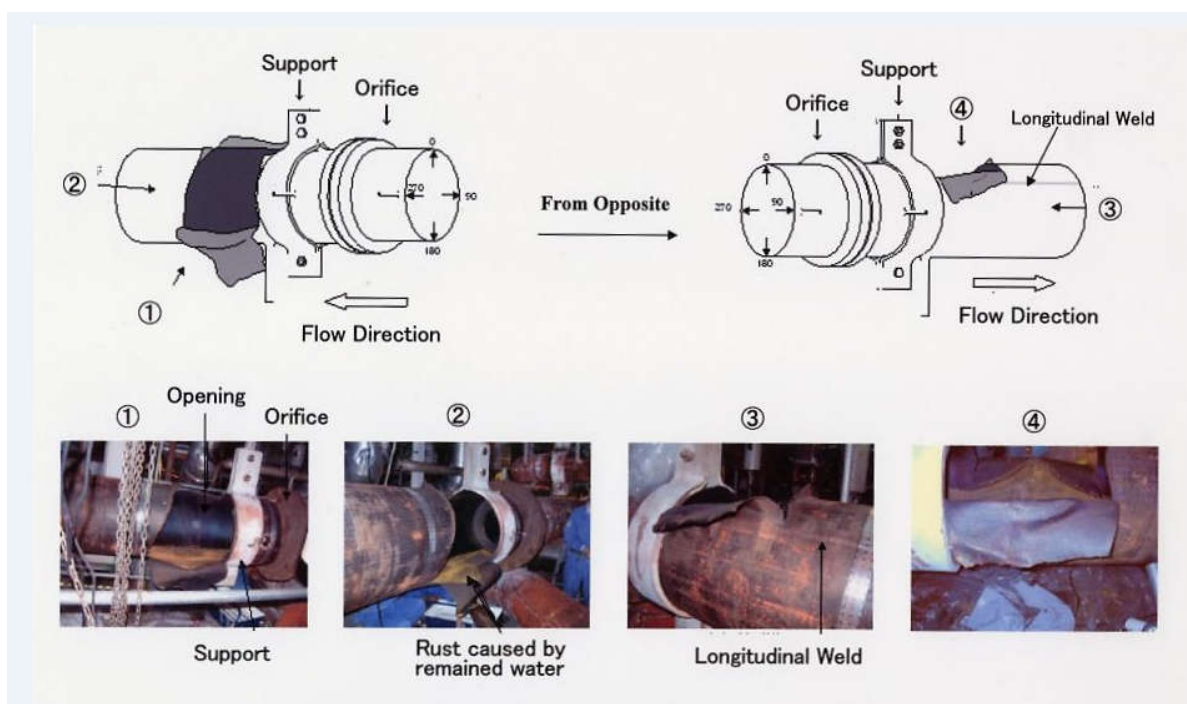

Figure 2.5. Point of Mihama rupture. (WANO report EAR TYO 04-013.)

Indian Point Unit 3 2018. Through-wall leakage on a 150 mm elbow's extrados on a steam-condensate pipe. The elbow located after a level control valve in a pre-heater condensate line containing steam-water mixture. Consequence of the leak was a manual reactor scram and loss of 375 GWh production. Investigation confirmed severe wall thinning around the elbow, minimum measured was 3,3 mm and the cause of the thinning was flow accelerated corrosion. After the incident similar location in parallel trains 43 additional component were inspected from which 9 was replaced due to FAC degradation. Figure 2.6 shows clearly a wall thickness difference on elbow's extrados and intrados. Interesting about this event is that the plant is using CHECWORKS model to predict the location where the FAC might cause wall thinning. Based on the model, plant has created a maintenance and inspection program to ensure these kind of events does not happen. Unfortunately, model was too simplified on this part of the piping and it was not taken into inspection program.
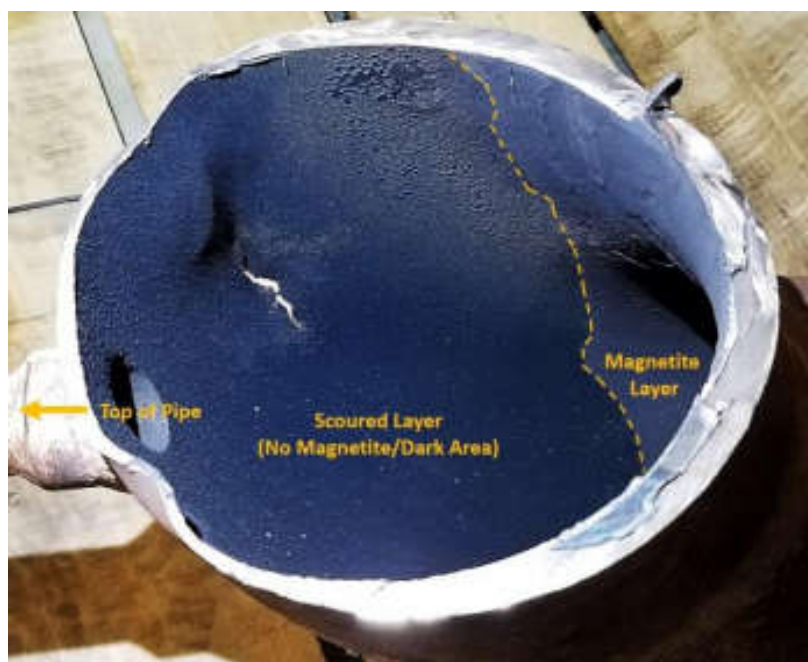
Figure 2.6. Corroded elbow showing wall thinning on extrados. (WANO report WER ATL 19-005.)

Now we know the basics of the electrochemical corrosion and what might be the results if it is not considered in the maintenance programs. In the next chapter the Flow Accelerated Corrosion phenomena is explained. The FAC is the based on the electrochemical corrosion induced by the flow and a root cause for the incidents listed in the chapter 2.

The importance of FAC awareness does not lie alone on the unplanned shutdowns that will lead to production losses or to the personnel safety. These are important for the plant owner and operator, but one aspect has not covered yet in this chapter. This is the reputation harm to the whole nuclear power industry. The industry is heavily regulated and any bad news have impact on the people mindset about the nuclear power. If majority of the people considers nuclear power unsafe to be used for the electricity production, the new plants will not get the construction permits and as in the Germany, even the old plants can be closed before the operation license end.

The nuclear power industry has spent a lot of time and effort to prove that the nuclear power is clean, safe and especially carbon free method to produce electricity. Any negative news from nuclear power plant causes media coverage and degrease the appreciation of the industry.

But of course, the problems caused by the FAC is borne by the operator and it is in their interest to know where and when the problems might occur.

3   FLOW ACCELERATED CORROSION

Flow accelerated corrosion or FAC phenomenon is a result of increase in the rate of corrosion or material dissolution. This increase is induced by relative moment of corrosive fluid on metal surface. It's important to note that when talking about FAC, it's always electrochemical effect, as described in chapter 2, not erosion caused by cavitation or water droplet impingement.

3.1   Flow Accelerated Corrosion mechanism

Within time, the process pipes on power plant forms a protective oxide layer on the surface of the pipe or equipment. This protective oxide limits the Fe^{2+} ions dissolution into the bulk water. The protective oxide film formation and thickness depend on ratio between rate of formation and rate of dissolution of the protective layer.

Figure 3.1 shows the mechanism of formation and dissolution of the iron oxides into the bulk water. The point number 1 show the steel corrosion at the metal-oxide interface. The point number 2 show soluble species diffusion inside porous oxide and the diffusion of the hydrogen through the steel. The point number 3 shows the oxide growth on a metal/oxide interface and reductive dissolution of oxide by hydrogen at the oxide/water interface. The point number 4 show mass transfer into the flowing water.
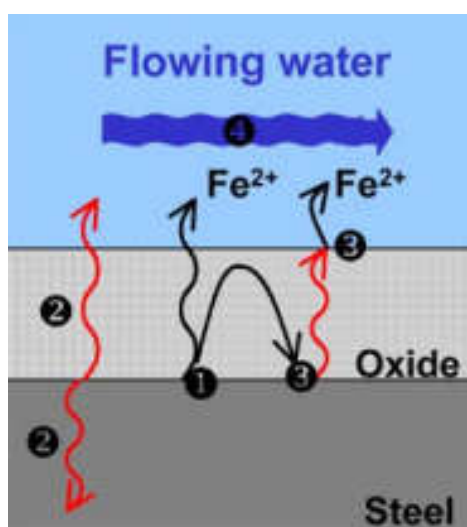
Figure 3.1 Protective oxide layer and the dissolution through it. (Gipon & Trevin 2020, p. 238.)

High FAC rates occur on a turbulent flow conditions that can be found on elbows, T-pieces, after orifice plates or even on a weld. At these highly turbulent locations, the film is dissolved more rapidly, and it's restoration become impossible. (Gipon & Trevin 2020, p. 230 – 243.)

The higher the flow speed of the water, the higher the turbulence that enhance the FAC process. The turbulence flow reduces the oxide layer thickness and enhance the corrosion process. Therefore, FAC might not be a problem for most part of the piping/equipment but can cause severe thinning on a more turbulent location.

3.2   Factors affecting FAC severity

There are several factors that are affecting the FAC rate. Experiments and data collected on an operating plant shows that water chemistry, temperature, hydrodynamic factors (turbulence) and the steel composition plays an important role when assessing FAC severity. (Gipon & Trevin 2020, p. 213-250.)

3.2.1   Water chemistry

Water chemistry effect can be expressed by pH and content of species which can influence on protective film formation/dissolution. The magnetite layer enabled to be produced on an iron when the water in contact with the metal is either neutral or alkalinized. The relative corrosion rate for an iron in an oxygen free water is lower for $pH_{25°C}$ in the range of 7 to 12 and higher for $pH_{25°C}$ less than 7 or higher than 13. At these lower or higher than $pH_{25°C}$ 7-12 values the oxide film becomes more soluble. This can be seen from the figure 3.2. The diagram is called as Pourbaix diagram and this specific diagram is for iron. From this diagram it's easy to check if there's a change for corrosion based on the equilibrium potential.
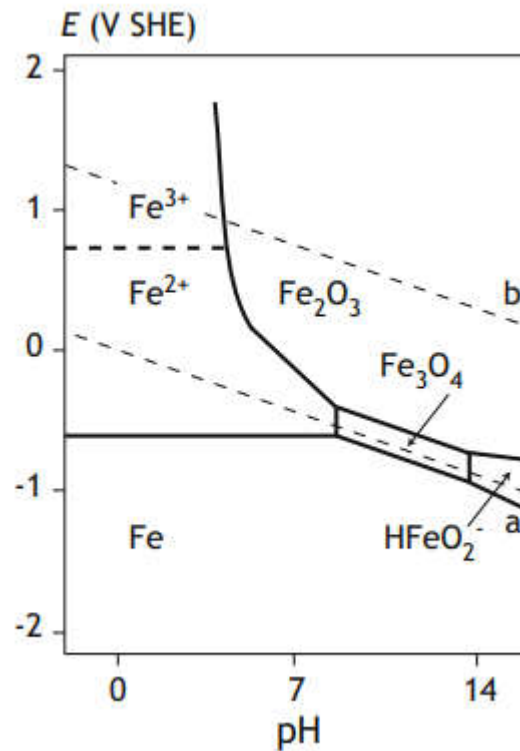
Figure 3.2 Pourbaix diagram for iron (Gipon & Trevin. 2020, p. 65.)

This is why pressurized water reactors secondary circuit typically has $pH_{25°C}$ value between 9-10. Studies have shown that the alkalizing agent does not play significant role in FAC process but the actual pH value does as can be seen in figure 3.3. Figure shows how dramatic effect pH and temperature can have on magnetite solubility. For example at 25 °C degree water has 1000 time lower solvent ability when pH is increased from 8 to 10.
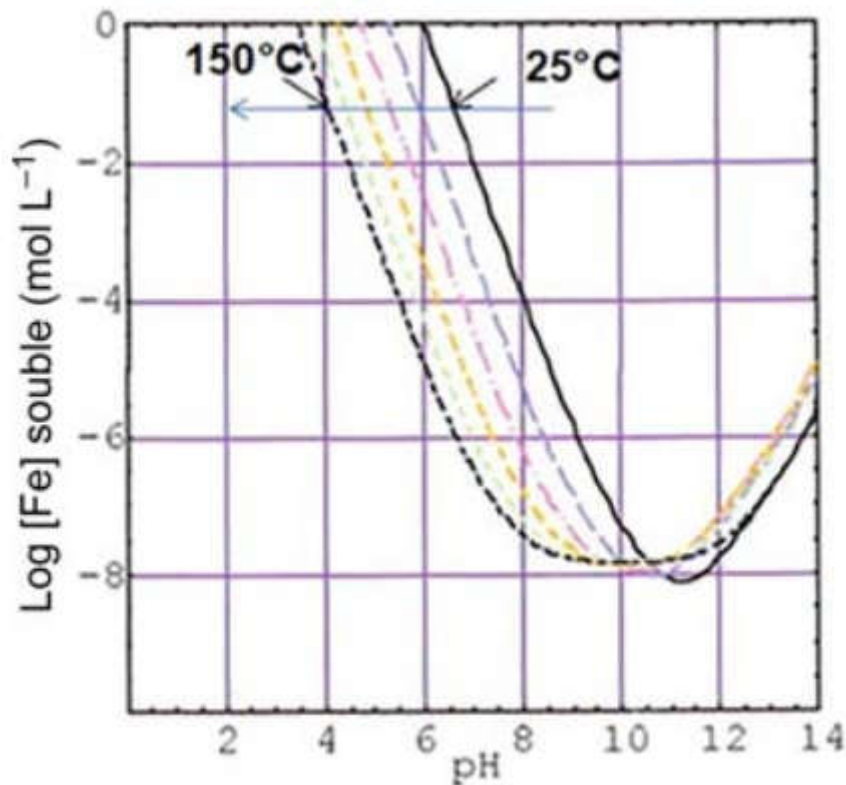
Figure 3.3. Magnetite solubility with different pH values. (Gipon & Trevin 2020, p. 225.)

The water content effect can be expressed mainly by Oxygen content, since in one hand Oxygen directly takes place in the protective film type and formation and in the other hand can have detrimental effect, if presented in a high concentration.

Most of the PWR's use hydrazine as an oxygen scavenger to keep the oxygen content in the feedwater lines as low as possible. Systems where the corrosion is under the control of oxygen reduction reaction (equation 2.3), the corrosion rate can be significantly influenced with the reduction of the oxygen content. It is also important to note that the oxygen amount in the flowing water affects the oxide layer type. In low oxygen levels for example when using hydrazine, the oxide film is made of magnetite (Fe_3O_4) and when the there's added oxygen of 10 mg/kg the oxide layer is formed from hematite (Fe_2O_3). Hematite is less soluble than the magnetite and enhance the resistance to FAC dramatically, practically halts the FAC process for unalloyed steel. (Gipon & Trevin 2020, p. 213-250.)

Other water characteristic, which can affect FAC rate is its conductivity. The Conductivity has a direct influence on corrosion rate when the cathodic process is present. In case of

Nuclear Power Plant (NPP) secondary side, the conductivity is kept as low as possible to prevent the localized corrosion, especially in the steam generators where the impurities finally concentrate. (Pedeferri 2018, p 124-125.)

3.2.2 Temperature

Temperature is one of the key factors affecting FAC rate on a carbon- and on a low-alloy steels. It is measured that the FAC occurs in the temperature range of 100-280 °C and peak corrosion rate is at 150 °C, as seen in the figure 3.4. With higher temperature the ferrous iron concentration decreases. This implies that with lower temperature the FAC rate should be at maximum level but the temperature also affects the flow viscosity and the ferrous iron diffusivity. Figure 3.4 shows the effect of the temperature on FAC rate. Left figure 3.4a shows corrosion rate that is measured after orifice plate with different flow speeds and at $pH_{25°C}$ 9,04. It clearly shows how the corrosion rate increase when the flow speed increases. For higher temperatures the corrosion rates are significantly lower in overall but with the higher flow speeds the corrosion rate is still significantly higher than with lower flow speed.

The right figure 3.4b is with stable flow parameters but with different materials. Flow speed is selected to be 35 m/s which is a high value for typical process piping. Purpose for the high speed is to get the test results quickly. This figure shows the effect of a materials. When the chrome and molybdenum content increase the corrosion rate decreases. (Gipon & Trevin 2020, p. 213-250)
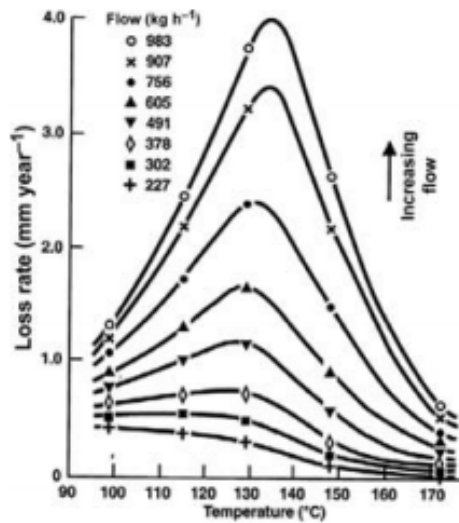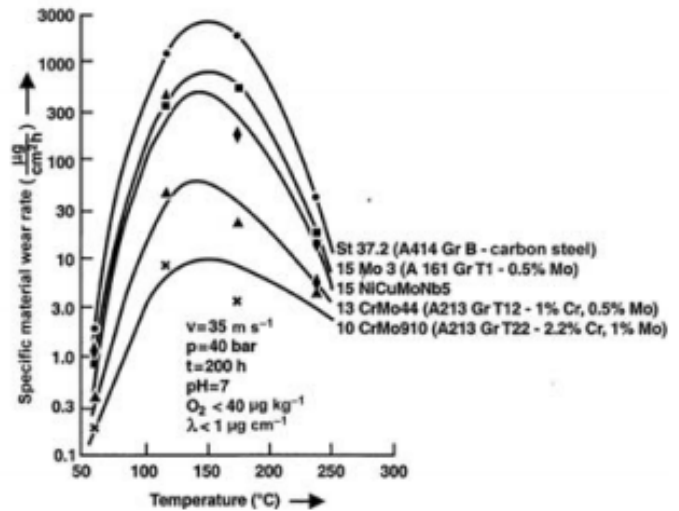
Figure 3.4a   Figure 3.4b

Figure 3.4. Temperature effect on a FAC rate. (Gipon & Trevin 2020, p. 228.)

3.2.3 Mass transfer conditions

Essentially FAC is a limited by the rate of mass transfer from the oxide layer. The term mass transfer facilitates the diffusion process of soluble species from the oxide layer to the flowing water in a pipe. Variables affecting mass transfer efficiency are flow speed, surface roughness, geometry of the pipe and for the two-phase flows also the steam quality and void fraction.

Higher flow speed leads to higher Reynold's number that means more turbulent flow. In heat exchanger this is favorable because it enhances heat transfer efficiency. But in a pipe, it causes higher pressure loss and increase dissolution rate. This can be seen from figure 3.4 (a). When mass flow increases from 491 kg/h at 130 °C to 983 kg/h at the same temperature the corrosion rate is almost four times greater. Also, the surface roughness and pipe geometry increase the turbulence in the flow significantly, especially the later one. This will be taken into account when calculating corrosion rates in chapters 4 and 5.

The flow rate has been found to have linear effect on a FAC rate. Higher the flow speed, higher the turbulence and higher the FAC rate. This is due to enhanced mass transfer efficiency. That is why the effect of the flow speed is often described in terms of mass transfer efficiency, which is a function of flow speed and pipe geometry. The local flow

velocities can differ by a factor of 2 to 3 from the bulk flow velocity. (Gipon & Trevin 2020, p. 227-229.)

3.2.4 Materials used

Steal composition plays an important role when estimating FAC rate. It is well known that the chromium, copper and molybdenum are good inhibitors for FAC. From these three the copper is the only additive you can not find from power plant process equipment. This is because the dissolved copper will deposit on turbine blades causing additional down time for the unit to clean the blades. It can be seen at Figure 3.4 (b), that at the same flow conditions, when the chrome and molybdenum content increase the corrosion rate decreases. Chromium and molybdenum can be found process equipment and especially chromium is used as additive to prevent the FAC to occur. Figure 3.5 shows how the relative FAC rate decreases on a logarithmic scale when the chromium content exceeds 0,04 %. It's important to note that even a small amount of chromium has impact on FAC rate as long as it is higher than the 0,04 % threshold value. Other important factor is that it decreases FAC rate also in case of two-phase flow. This is demonstrated in figure 3.5 by the red symbols, circle values are for lower flow speed with steam content of 80 % and the square symbol for higher flow speed with a steam content of 64 %.
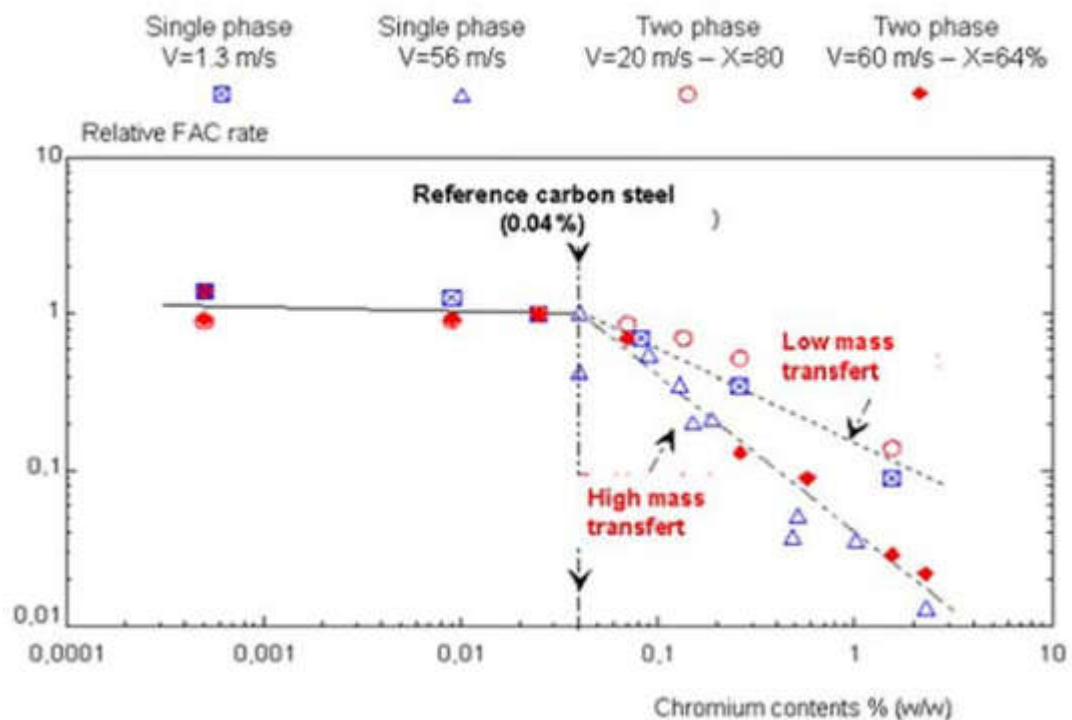
Figure 3.5. Effect of chromium content on a FAC rate. (Gipon & Trevin 2020, p. 241.)

3.2.5 Geometry

The surface roughness and pipe geometry increase the turbulence in the flow significantly, especially the second one. Any flow restrictors cause turbulence and therefore will increase the mass transfer from the oxide layer. It's important to note that any single restrictor can have significant impact on corrosion rate but also if they are located near each other, they first one will enhance the impact after the second one if the distance between them is not enough for the flow to return to normal flow conditions. The type of the restrictor impact the turbulency as can be seen from table 4.2 where the Keller coefficient are listed for various restrictors. It's important to note that the smaller the elbows bend radius, the higher the Keller coefficient and higher the corrosion rate. (Gipon & Trevin 2020, p. 227-229.)

Typically, this is considered when having a greenfield project but in case of a brownfield project the existing lay-out will limit the pipe routing and sizing. This will be considered when calculating corrosion rates in chapter 4 and 5.

3.3 Existing flow accelerated corrosion models

There are several computer programs that are used to estimate FAC rate in power plants and generally in process industry. Development of these software started after the Surry accident when operating plants realize FAC has not been taken into account in inspection- or in maintenance plans. Concern over personnel health and sudden production loss initiated predictive FAC calculation model development. Today the tools are used to estimate plant life time and to pinpoint exact location to be taken into inspection programs, for example the areas that are more prone to corrosion will be inspected more frequently. Next chapters give basic information about the existing models.

CHECWORKS from Electric Power Research Institute. The model takes into account geometrical factors, pH, oxygen content, material properties, temperature, void fraction, hydrazine concentration and mass transfer effect. Model is optimized by comparing predictions made with the software to the actual wear rate. (Feron 2012, p 218-222.)

Framatome COMSY code. This software tool was originally developed by Siemens in 1980's and were transferred to AREVA in 2001 and later to Framatome. The model takes into account geometrical factors, fluid velocity, pH, oxygen content, material properties and temperature. The difference to the CHECWORKS is hydrazine concentration, that affect the oxide porosity, void fraction that is used for two-phase flows and mass transfer effect that is replaced with flow speed. Software can be called semi-empirical model since the basis are the same as for the CHECWORKS model integrated with the Keller's geometry factor. Empirical part comes from the extensive laboratory test and from the real-life data collected from operating plants. Model is corrected based on the data with correlation factors. (Feron 2012, p 218-222.)

BRT-CICERO from EdF. CICERO codes take into account pH, oxygen content, temperature, material properties, and mass transfer coefficient. Model is verified with results from a laboratory test and with the data collected from the power plant. In a year 2000 software enabled operator to detect severe wall thinning after a control valve on Fessenheim power plant, EdF decided to take CICERO in use in all its 58 nuclear power plants. (Feron 2012, p 218-222.)

What is common to these models is that the calculation programs are modified with real corrosion rate data collected from the operating plants and from an extensive laboratory test. This indicates that the original calculations made by the programmers did not give the same results as was measured from the operating plant. This is understandable if you consider how many variables there are and how, or to what extent, they will affect the corrosion rates. Therefore, it's practically impossible to calculate corrosion rate correctly or to create a universal calculation program for every situation. There are always some changes in flows, or in temperature, or in chemistry that affect the real corrosion rate. However, these initial theoretical calculations, are used to define the places more prone to suffer from FAC and to include them in inspection activities.

The calculation models listed above, do not present detailed information, how the factors affecting FAC are considered but it shows the parameters used to estimate it. In aim to clarify a bit this question, development of simplified model for calculation of FAC rate is described in the next chapter.

4   METHOD FOR CALCULATION FAC SPEED

This chapter gives information how the calculations in the present Master thesis are done and what kind of variables there are when estimating FAC rate. For single phase flow an equation have been chosen to be used so that all the needed information to perform the calculations are available. This is a simplified model because the information from the existing plants or from the laboratory test performed by companies mentioned in chapter 3.3 are not available at this stage.

In aim to take into account the factors which have significant effect of FAC at different environmental conditions, it was decided to use two different approaches for calculate FAC rates in single- and two-phase flow conditions.

Suitable equations to start are taken from for one phase flow (Gipon & Trevin 2020, p. 233). and from for two phase flows. (Delp. 1985 p. 2-20).

Despite taking several factors into account, some factors have been left out from equations. First one is oxygen content in the water. As explained in chapter 3.2.1 the oxygen content will affect the FAC rate and in typically increase the corrosion rate when the oxygen content increases. On the other hand, it can have reducing effect as in boiling water reactors with neutral pH feed water and with hydrazine as an additive. However, in NPP secondary circuit Oxygen content is controlled to be constant and low enough, so in this why it will not have significant effect on FAC rate. The additives are the second factor not taken into account. This applies especially to the hydrazine that has a big impact on the protective oxide film formation and type. The exact additives used to control pH level does not have direct impact on corrosion rates, thus the calculations are based only on pH level. The third factor not considered in calculations is the conditions of the oxide film and the type of it. The film can be thin or thick, dens or porous or perhaps it's not yet even formed yet. That is why the corrosion rate is higher when the unit is commissioned and decrease when the protective oxide layer is formed. In the present calculation the oxide film thickness and type are considered constant and the calculated result presents corrosion rate average value. Related to this, also the erosion of the film, or the base metal itself is not considered, since wall

thinning caused by erosion is not considered. For the flow restrictors such as elbows and T-pieces, only one correlation factor has been considered in the calculation. In reality there might be several pieces causing flow disturbance in a row with a short distance from each other. Therefore, there are some turbulence left from the previous flow restrictor that should be taken into account when defining the coefficient for the restrictors. Addition for these in the two-phase flow calculation, the effect of pH is not considered since the corrosion rate is mainly affected by the moisture content.

4.1   Single phase flow calculation method

Based on the publications listed above, single phase FAC rate can be calculated as a function of iron ions (Fe^{2+}) concentrations at the oxide surface in contact with the environment and Fe^{2+} concentration in the flow.

$$FAC_{rate} \; = \; k \; (C_s \; - \; C_\infty), \; \left[\frac{kg}{m^2 s}\right] \tag{4.1}$$

The equation 4.1 also includes mass transfer coefficient, k. Where C_s stands for Fe^{2+} concentration at the surface of the water oxide interface and can be equated with the Fe^{2+} concentration corresponding to the equilibrium oxide solubility, presented on figure 4.1, C_∞ is the Fe^{2+} concentration in the flow. In aim to apply more conservative approach, it is assumed that all dissolved Fe^{2+} ions are taken away by the flow and so $C_\infty = 0$.
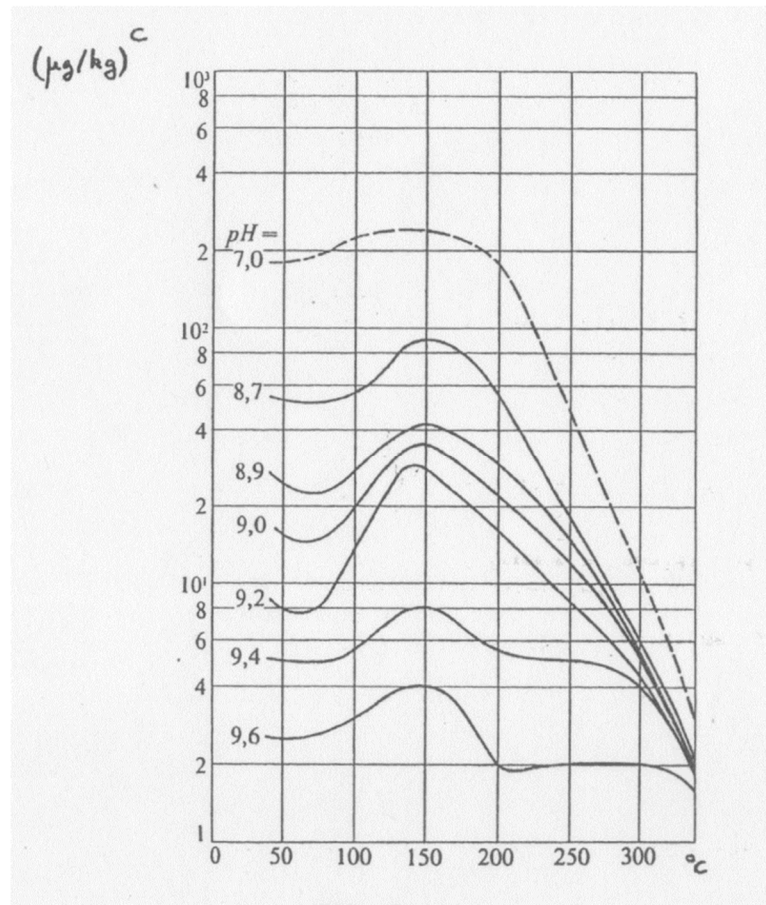
Figure 4.1 Equilibrium oxide solubility (Fe^{2+} concentration) as a function of temperature and pH. (Goffin 1990, p. 44.)

In the other hand, mass transfer coefficient k, can be expressed by:

$$k = Sh\frac{D}{d}, \left[\frac{m}{s}\right] \tag{4.2}$$

Where **Sh** stands for Sherwood number, **d** - pipe diameter (m) and **D** – diffusivity of Fe ions, (m^2/s).

Combining equations 4.1 and 4.2, FAC rate can be expressed by:

$$FAC\ rate = Sh \cdot \frac{D}{d} \cdot (C_s - C_\infty), \left[\frac{kg}{m^2 s}\right] \tag{4.3}$$

The Sherwood number is dimensionless and describes the mass transfer from the metal to the flow.

$$Sh = 0{,}0165 \cdot Re^{0,86} \cdot Sc^{0,33} \tag{4.4}$$

In the literature, there are several different equations for Sherwood number calculation, but the following equation 4.4 chosen, because it is valid for Reynolds numbers between 10^4 to 10^7 which is where most of the power plant process piping Reynolds numbers are.

$$Re = \frac{V \cdot d}{v} \tag{4.5}$$

The symbol $\boldsymbol{Re}$ is used for Reynolds number that is calculated by the equation 4.5. It is also dimensionless and gives information of how turbulent the flow is. Reynolds number is calculated by multiplying flow velocity, $\boldsymbol{V}$ (m/s) with pipe inner diameter, $\boldsymbol{d}$ (m) and divided it by kinematic viscosity, $\boldsymbol{v}$ (m²/s).

$$V = \frac{\dot{m}}{\rho . A}, \left[\frac{m}{s}\right] \tag{4.6}$$

The flow velocity is calculated in equation 4.6 by dividing the mass flow, $\boldsymbol{\dot{m}}$ (kg/s) by fluid density, $\boldsymbol{\rho}$ (kg/m³) and then dividing the result with the cross-section area, $\boldsymbol{A}$ in m².

$$Sc = \frac{v}{D} \tag{4.7}$$

The $\boldsymbol{Sc}$ term is the Schmidt number that is calculated by the equation 4.7. The Schmidt number takes into account the effect of temperature and interaction forces between steel surface and flow regime. In the equation the $\boldsymbol{v}$ is the kinematic viscosity. The Schmidt number is dimensionless.

Where $\boldsymbol{D}$ stand for diffusivity (m²/s) and for iron-soluble species it can be taken from the figure 4.2. The diffusivity is read from the figure as a function of temperature.
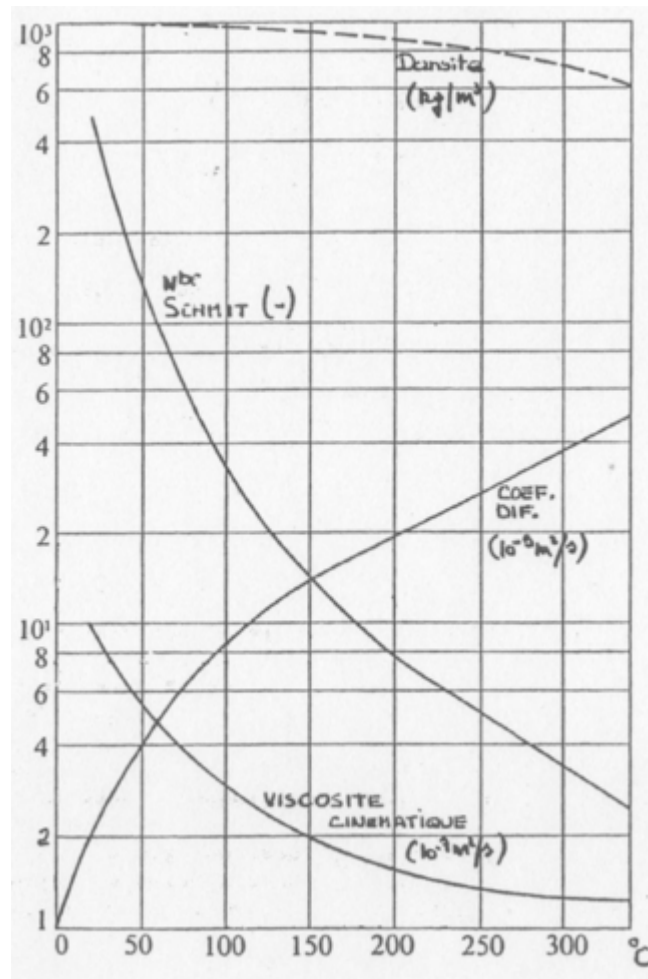
Figure 4.2. Schmidt number, Diffusivity coefficient, Kinematic viscosity, and water density as a function of temperature. (Goffin 1990, p. 44.)

Kinematic viscosity, Schmidt number and water density could be also taken from figure 4.2 but to get more accurate values, the earlier described equations are used in the calculation. Steam and water properties used in the calculation are taken from steam table IAPWS IF-97. These are physical properties of steam and water and are only affected by the pressure and temperature. Table 4.1 shows with grey color the properties taken from the tables as a function of pressure and temperature. Only exception is kinematic viscosity that is calculated by dividing dynamic viscosity with density of the water.

Table 4.1 Water properties used from steam tables

Pressure	bar(a)
Temperature	°C
Mass flow	kg/s
Cs surface concentration of iron	µg/kg
C∞ bulk concentration of iron	mg/dm³
Saturation temperature	°C
Specific volume	m³/kg
Density (g)	kg/m³
Dynamic viscosity (µ)	kg/(ms)
Kinematic viscosity (v)	m²/s

Corrosion rate calculated by equation 4.1 will refer to corrosion rate for a straight carbon steel pipe with no Chromium content. However, it is well known that most of the flow accelerated corrosion incidents occur after some flow restrictors, such as elbows, orifice plates or T-pieces.

$$\text{FAC rate (g)} = \text{FAC rate} \cdot \frac{k_c}{k_{cs}} \qquad (4.9)$$

Therefore, results are not representative without considering the most prone areas to the flow accelerated corrosion. This can be done by adding a Keller coefficient into the equation. Thus, the FAC rate considering geometry *FAC rate (g)* can be presented by dividing the chosen geometry coefficient, k_c by coefficient of a straight pipe, k_{cs} from table 4.2 and by multiplying the result with the calculated corrosion rate for a straight pipe as in the equation 4.9

Table 4.2 Keller coefficient used for calculation.

FLOW PATTERN			REFERENCE VELOCITY	K_c
PRIMARY FLOW STAGNATION POINTS	→ ◯	AT PIPES	VELOCITY OF INITIAL FLOW (UPSTREAM OF STAGNATION OBSTACLE)	1
	→ ⊃	AT BLADES		1
	→ ⌐	AT PLATES		1
	⊤	IN PIPE JUNCTIONS		1
	⊥			0.8
SECONDARY FLOW STAGNATION POINTS	→ ⌐	$R_{MEAN}/D = 0.5$	FLOW VELOCITY	0.7
	→ ⌐	$R_{MEAN}/D = 1.5$	IN ELBOW PIPES	0.4
	→ ⌐	$R_{MEAN}/D = 2.5$		0.3
	⊤	BEHIND PIPE JOINTS		0.2
	⊤			
STAGNATION POINTS DUE TO VORTEX FORMATION	⊥	BEHIND SHARP EDGED ADMISSION PIPES	FLOW VELOCITY	0.2
	→	AT AND BEHIND BARRIERS		0.2
NO STAGNATION POINTS	→	IN STRAIGHT PIPES	FLOW VELOCITY	0.04
	═══	IN UNTIGHT HORIZONTAL TURBINE JOINTS	VELOCITY CALCULATED FROM PRESSURE DROP	0.08
COMPLICATED FLOW THROUGH TURBINE PART	⊥⊥⊥⊥⊥	IN TURBINE GLAND SEAL	VELOCITY CALCULATED FROM PRESSURE DROP	0.08
	⌐	AT AND ABOVE TURBINE BLADES AND AT DRAINAGE COLLECTING RINGS	AVERAGE CIRCUMFERENTIAL BLADE VELOCITY	0.3

As written above, equation 4.1 also does not take the material effect into account. Figures 3.4 and 3.5 shows how the corrosion rate can differ by changing the material of the pipe when having otherwise the same process parameters.

$$FAC = FAC_{rate\ max} * \frac{1}{83*[Cr]^{0,89}+[Cu]^{0,25}+[Mo]^{0,2}}$$ (4.10)

The material effect can be estimated by using the Ducreux relationship shown in equation 4.10. The FAC $_{rate\ max}$ stands for the calculated maximum rate for carbon steel pipe, or to be more precise, for pipes that has chrome content lower than 0,04 wt% threshold value described earlier in chapter 3.2.4. Chrome, copper and molybdenum content should be given as weight percentage.

As it can be seen from equation 4.10 the biggest effect for limiting FAC rate is the chrome content and since the copper is not allowed to be used in secondary circuit and the molybdenum content is typically small for the process equipment it can be assumed that the chromium content has biggest impact on FAC rate. This can be confirmed from Figure 4.3 that shows how the FAC rate decreases when the chromium content increase. The biggest corrosion rate reduction happens when chromium content increases from 0,04 to 0,2% and the corrosion process is insignificantly small when chromium content is more than 1 %. This is also a reason why stainless steels (Chromium content more than 12 %) are not prone for flow accelerated corrosion but they can suffer other type of corrosion failures as described in Chapter 2. (Gipon & Trevin 2020, p. 222-230.)
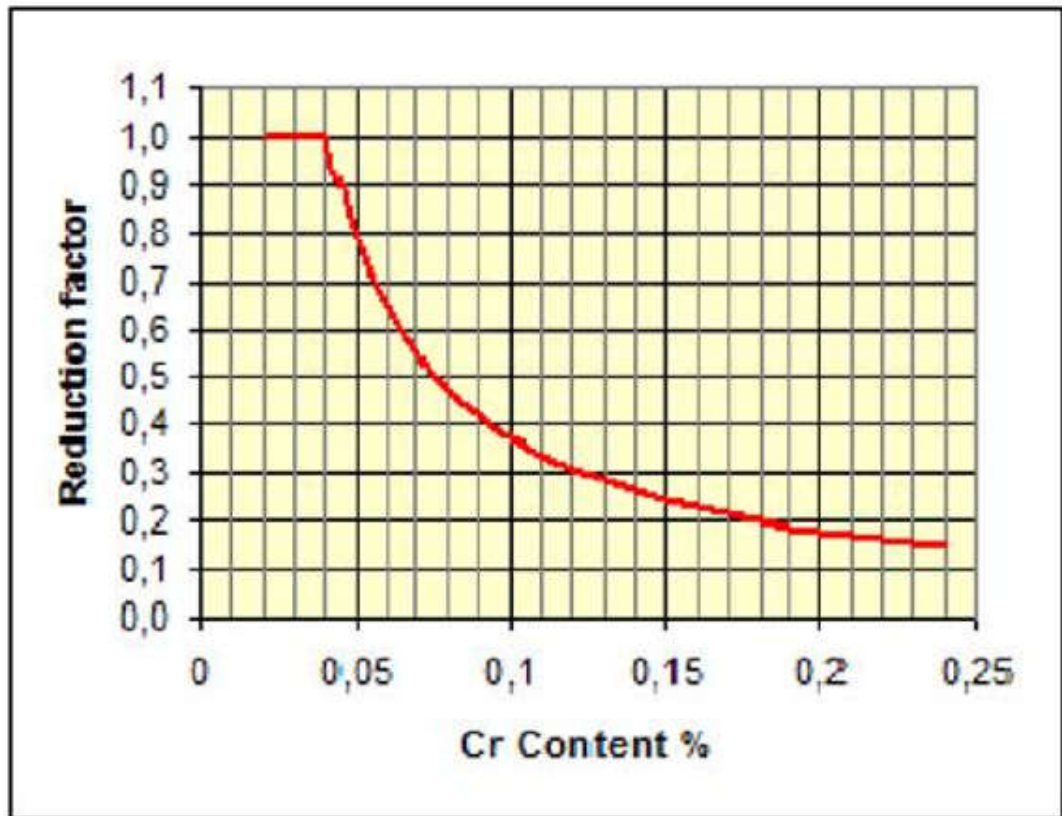
Figure 4.3. Chromium content effect to FAC rate. (Trevin 2012, p. 5.)

The problem with the equation 4.10 is that the relative corrosion rate decreases dramatically when the Chromium content increases from 0,04 % threshold value. The difference to the figure 4.3 seems to get smaller on a higher Chromium contents. Problem is that the typical pressure vessel steel does not contain high concentrations of Chromium, therefore this formula is not applicable for calculation FAC material reduction factor for power plant piping. Instead in our calculation, we have used the reduction factor from the figure 4.3. This is for both, to be more conservative in the calculations and in other hand, not to have different factors that have been tested and proven to be correct in practice. And as described earlier the Copper is not applicable to power plant piping and the Molybdenum is typically used as additive in metals to have better high temperature properties in steal. Therefore, these can be neglected from the calculation.

Since equation 4.1 represents the FAC rate in $\left[\frac{kg}{m^2 s}\right]$, conversion factors presented in chapter 2.1 are used to convert it in $\left[\frac{mm}{yr}\right]$.

With these equation and input data we created the excel based calculation tool. The picture of it is shown in table 4.3. There the yellow cells are the input parameters and the blue cells are the results. The grey cells are calculation steps or physical properties of water and they are used with the input data to calculate the blue cells.

Table 4.3. Calculation excel for single phase flow

						1 year	60 years
Pressure	bar(a)	70	Water				
Temperature	°C	150	IAPWS IF-97 steam tables				
Mass flow	kg/s	715					
Cs surface concentration of iron	µg/kg	250	in kg/kg	2,50E-07			
Cl bulk concentration of iron	mg/dm³	0	in kg/m³	0,00E+00			
Saturation temperature	°C	286					
Specific volume	m³/kg	0,001086169					
Density (g)	kg/m³	920,6674034					
Dynamic viscosity (µ)	kg/(ms)	1,836E-04					
Kinematic viscosity (v)	m²/s	1,995E-07					
Pipe outer diameter	mm	465	in m	0,465			
Wall thicness	mm	30	in m	0,03			
Pipe inner diameter (d)	mm	405	in m	0,405			
Flow area	m²	0,128825					
Flow speed (V)	m/s	6,0					
Reynolds number (Re)		1,224E+07					
Schmidt number (Sc)		1,330E+01					
Sherwood number (Sh)		4,829E+04					
Diffusivity (D)	m²/s	1,500E-08					
Metal density (ρ)	kg/m³	7800				1 year	60 years
FAC (for carbon steel)	kg/m²s	4,47E-10	in mm	5,73E-11		1,81E-03	1,08E-01
FAC with Keller (carbon steel)	kg/m²s	4,47E-09	in mm	5,73E-10		1,81E-02	1,08E+00
Material effect:	Cr%	0,100					
	Cu%	0,0					
	Mo%	0,0					
		10,69					
						1 year	60 years
FAC with material	kg/m²s	4,78E-09	in mm	6,13E-10		1,93E-02	1,16E+00
		9,35E-02					
Kc		0,4					
Kcs		0,04					
Keller coefficient		10,00					
						1 year	60 years
FAC with Keller and material	kg/m²s	4,78E-08	in mm	6,13E-09		1,93E-01	1,16E+01

4.2 Two-phase flow calculation method

For the two phase flows the same steam parameters are used as for the one-phase flows and they are taken from the same IAPWS IF-97 steam tables as in case of one-phase flow. Only addition is the steam fraction (x) that describes how dry the steam is. For example, for fully saturated steam, or super heated steam, the steam fraction is 1, but when the moisture content

increase in saturated steam, the steam content decrease. This has a significant impact on FAC rate as we can see in the following chapters.

For calculation of corrosion rate in two-phase flow conditions, Keller equation is to be used.

$$FAC_{straight} = f(t) * f(x) * V * K_c - K_s \ \frac{mm}{10^4 h} \tag{4.11}$$

Keller equation is presented in equation 4.11. Corrosion rate measurement units in this case are millimeters for 10^4 hours.

The function f(t) gives correlation factor takin into account the temperature as shown in figure 4.3. The graph will give the dimensionless temperature coefficient to be used in calculation.
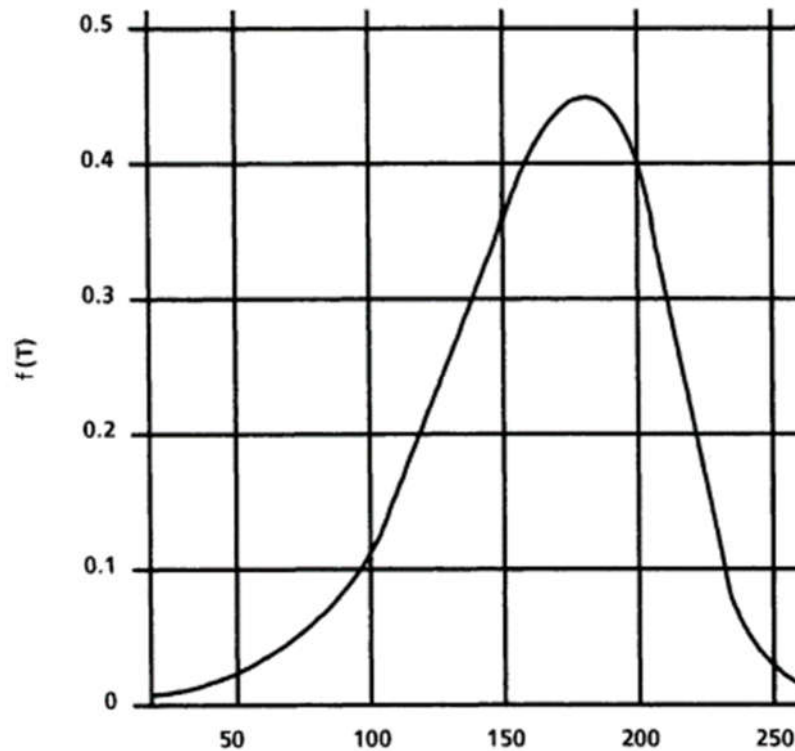
Figure 4.3 Correlation factor for temperature in two-phase FAC calculation (Delp 1985 p. 37.)

$$f(x) = (1 - x)^{\wedge}K_x \tag{4.12}$$

The function f(x) Is dimensionless value denoting the steam dryness. Function *f(x)* is described with the equation shown in 4.12 where the x is equal to the steam content in decimal. For example, if the steam has 2% moisture content, then the steam content is 98%, therefore *x* is 0,98. The term K_x has a value bigger than 0 and smaller than 1. This term can be used to change the effect of moisture content in the calculation if there is data available from a laboratory test or from operating plant. If these are not available, then the value of 0,5 has been considered the most appropriate one. Since there are not data available to be used in the present calculations, value 0,5 is used.

The variable V (m/s) is the flow speed and it is calculated same way as for single phase flow. The K_c variable is for local geometry effect (mm s/m 10^4h). This local geometry effect variable, or so called Keller coefficient can be taken from table 4.2. At this stage, the coefficient for the straight pipe is to be used.

The variable K_s is a constant threshold value of 1,0 mm/10^4h. This value has been set as a minimum corrosion rate to be exceeded before the FAC is observed. This means that if the result is negative, then the FAC phenomena is not observed.

The equation 4.12 takes only into account the straight pipe. As already described earlier, the FAC phenomena occurs mostly in places where are flow restrictors such as elbows or T-pieces.

$$FAC_{Keller} = \frac{K_c}{K_{cs}} \left(FAC_{straight} + K_s \right) - K_s \qquad (4.13)$$

To take this into account we need to apply a new variable into the equation. This variable is a relationship of the Keller variable between straight pipe and chosen geometry factor. This relationship is shown in equation 4.13.

The term K_c the specific Keller coefficient for chosen geometry and K_{cs} is for straight pipe. The $FAC_{straight}$ is the result from FAC rate for straight pipe and K_s is the same minimum value for corrosion rate as in equation 4.12. The Keller coefficient values are taken from table 4.2.

The equation 4.13 gives FAC rate for the carbon steel piping only, so to take into account the material effect, the same reduction factor is used as in the equation 4.10. Since by Keller equation the FAC rate is calculated for mm/10^4h, in created Excels the rate is additionally recalculated for longer period (as example, 60 years).

With these equation we created the calculation excel tool for two-phase flow. This can be seen in table 4.4 where the yellow cells are the input parameters and the blue cells are the result lines. The grey cells are physical properties of steam or water and calculation steps that are used in the FAC rate calculation.

Table 4.4 Calculation excel for two-phase flows

Pressure	bar(a)	15	Steam	
Temperature	°C	200	IAPWS IF-97 steam tables	
Mass flow	kg/s	45		
Saturation temperature	°C	198		
Specific volume	m³/kg	0,132440954		
Density (g)	kg/m³	7,550534532		
Dynamic viscosity (μ)	kg/(ms)	1,579E-05		
Kinematic viscosity (v)	m²/s	2,092E-06		
steam fraction (x)		0,95		
Pipe outer diameter	mm	465	in m	0,465
Wall thicness	mm	30	in m	0,03
Pipe inner diameter (d)	mm	405	in m	0,405
Flow area	m²	0,128825		
Flow speed (V)	m/s	46,26		
Reynolds number (Re)		8,958E+06		
f(x)		2,236E-01		
Ks	mm/10000h	1,000E-04		
f(t)		0,40		
FAC straight pipe	mm/h e4	1,65E-01		
Kc		0,30 (elbow)		
Kcs		0,04		
FAC with Keller	mm/10000h e4	1,241E+00		
Material effect:	Cr %	0,500		
	Cu %	0,0		
	Mo %	0,0		
		0,02		
FAC with Keller and material	mm/10000h e4	2,771E-02		

5   CALCULATIONS

Earlier it was shown that the FAC rate is at the highest when the temperature is in 100 °C to 280 °C range and peaking at around 150 °C. This is valid for both one- and two-phase flows. For the two-phase flow the biggest difference to the one-phase flow is the moisture content in the steam, higher the moisture content, higher the corrosion rate. Since other variables affecting the FAC rate are same for both flow types, it's possible to estimate what are the most prone places for FAC in the nuclear power plant secondary circuit.

The figure 5.1 shows a typical process arrangement for a secondary circuit. With these types of heat balance diagrams, it's possible to pinpoint the location that are prone for FAC based on temperature and moisture content. Examples of flow accelerated corrosion incident given in chapter 2.4 are in typical places where you would expect to have corrosion problems. For example, Surry 2 incident happened in same part of the system as point number 1 in figure 5.1, in main feed water pipe before high pressure pre-heaters. Temperature before the high-pressure pre-heater is typically from 150 °C to 200 °C, depending on the feed water tank pressure. Also the pipe geometry contains T-pieces and elbows because there are several pumps needed to provide necessary mass flow to the steam generator, meaning that there's a need firstly to balance the flow from individual pumps in a pressure header and then dividing it to the high pressure heater streams.

Point number 2 is taken into this study because after the high-pressure pre-heaters the feed water goes through a control valve that creates additional turbulence, hence enhancing the FAC probability. To be noted that the temperature is high during normal operation, around 220 °C. This part of the piping is already nuclear safety classified therefore the nuclear safety authorities are more keen on knowing the potential hazards in this area.

The Mihama 3 incident was located in a point number 3 in figure 5.1. At this point of secondary circuit, the temperature range is from 120 °C to 160 °C and contain similar pipe geometry as described for feed water system.

The point number 4 is chosen because all the steam lines coming from turbine are typically very moist, except the ones right after the moisture separator re-heater where the steam is dry or even super heated. Before the MSR, the steam is very wet, moisture content from 5 to 10 % and temperature range is from 150 °C to 230 °C.

The point number 5 is where the moisture content is at highest, typically over 15 % and the temperature is close to 180 °C. Obvious place to have FAC problems based on the temperature and moisture content.

The point number 6 is chosen because of the possibility to have a flash steam in the pipe. This phenomenon occurs in places where the saturated condensate in a high pressure suddenly have pressure reduction, for example because of pressure difference after a control valve and part of the condensate will flash. This will create much higher flow speeds than in typical water pipe lines even though the steam content can be quite low. Since there are two-phases present, this location is calculated as a two-phase flow. There the moisture content is high, close to 99 % depending on a pressure difference over the control valve. Temperature in the drain lines can vary a lot depending what part of the process is under examination but in this calculation, we concentrate on most severe cases considering FAC, so the temperature is set to 180 °C.
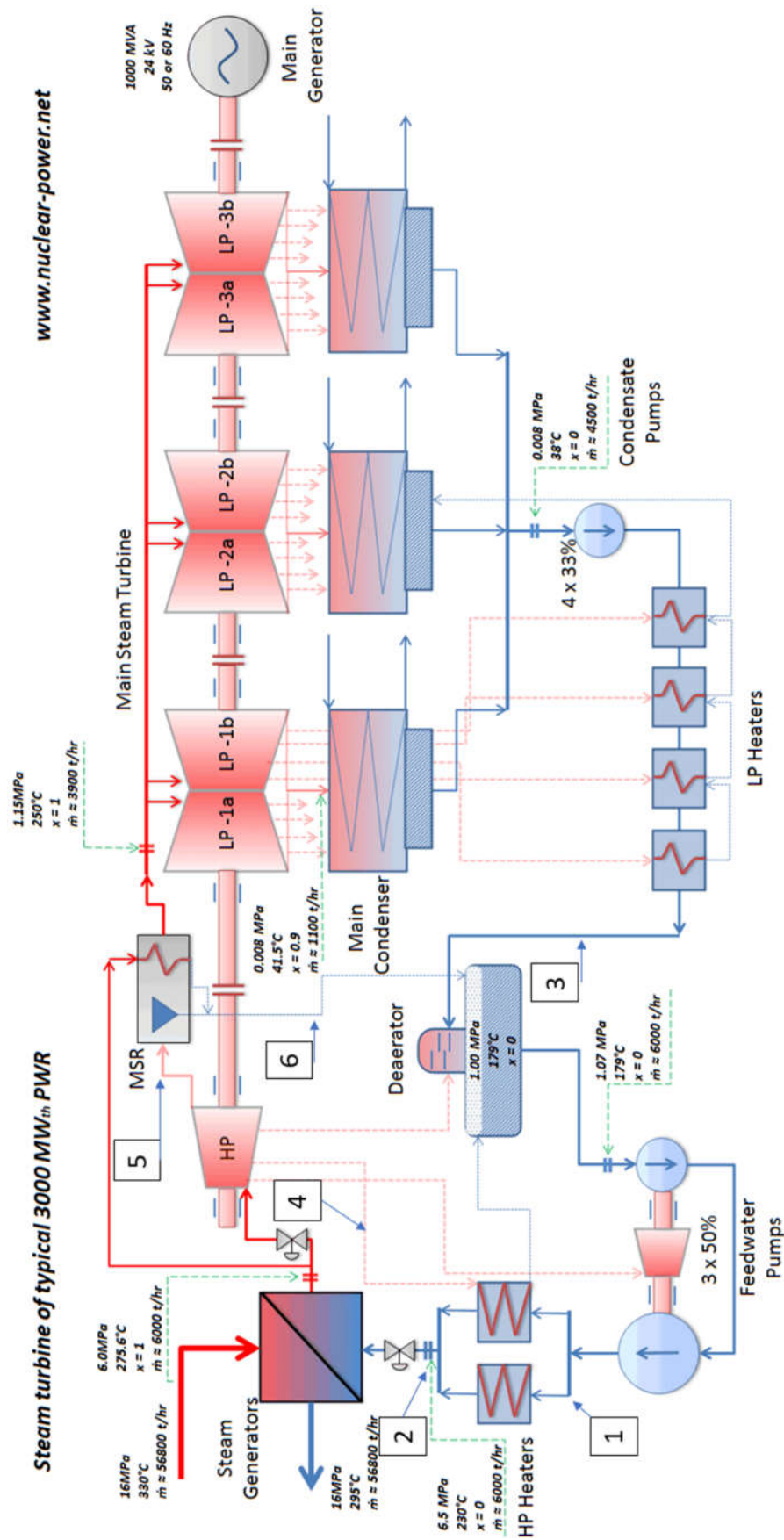
Figure 5.1 Typical secondary circuit flow diagram /*www.nuclear-power.net* /

5.1   One-phase flow calculation

Three different locations are selected to be examined for one-phase flow. The locations are selected based on the probability of the FAC to occur and partly because of safety perspective.

5.1.1   The point 1, feed water before pre-heaters

The point number 1 process parameters are chosen based on a typical feed water system values. Temperature is set to 180 °C. The temperature is depended on a pressure level on a feed water tank that slides according power level of the plant. Since the nuclear power plants typically operate as a base load plants with full power, other operating points are not considered.

The figure 5.2 gives calculated corrosion rates for fixed value of:

- Pressure 85 bar(a)
- Temperature 180 °C
- pH 9,6
- Iron surface concentration of 4,00E-09 kg/kg
- Diffusivity of 1,5E-08 m²/s
- Metal density of 7800 kg/m³

The numerical values are presented in Appendix 1. The blue line presents the calculated results for a carbon steel without alloying metals reducing corrosion rate for a straight pipe. The red line presents values for a same carbon steel pipe with a tight elbow. The green line present corrosion rate for a similar elbow but the pipe material contains 0,1 w% of Chromium. The red and green lines are for a similar pipe geometry and therefore easily comparable.

Results show how important it is to have a proper piping geometry. For example, the used long radius elbow (2,5 D) have 7,5 time higher corrosion rate as for a straight pipe. Equally important is to note that even 0,1 % of Chromium reduces corrosion rate significantly compared to the plain carbon steel.
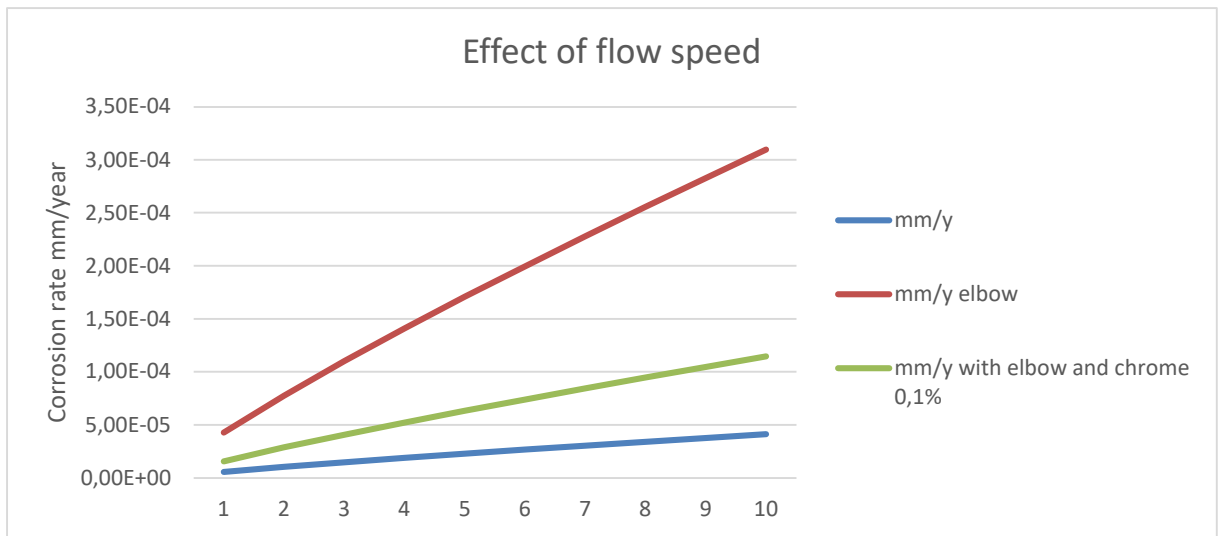
Figure 5.2. Flow speed effect on corrosion rate (pH 9,6 and 180 °C)

5.1.2 The point 2, feed water after pre-heaters

The point number 2 has typically similar piping geometry but the pressure level is a bit lower and the temperature is higher. In this calculation the pressure is 10 bar lower than in point one, now set to 75 bar(a) and the temperature is set to 220 °C. Decrease in pressure will have a small impact on a viscosity and to the density of the water but the difference is insignificantly small. Bigger impact is caused by the temperature increase. This will degrease density by 5 %, meaning that with the same mass flow the flow speed is higher. Temperature increases also the diffusivity. At 180 °C the diffusivity is 1,8E-08 and at 220 °C it is 2,5E-08. All these should increase the corrosion rate but based on the experiments and data collected from operating plants, the corrosion rate should degrease when temperature increases over 200 °C. The figure 5.3 presents the calculated corrosion rates with fixed values of:

- Pressure 75 bar(a)
- Temperature 220 °C
- pH 9,6
- Iron surface concentration of 1,95E-09 kg/kg
- Diffusivity of 2,5E-08 m²/s
- Metal density of 7800 kg/m³

The blue line is for straight carbon steel pipe, the red line is for elbow of a carbon steel pipe and the green line is for an elbow of a pipe containing 0,1 % of Chromium. The numerical values are presented in Appendix 1.

Figure 5.3. Flow speed effect on corrosion rate (pH 9,6 and 220 °C)

As it can be seen from the results the corrosion rates are smaller for similar piping geometry with similar properties when the temperature increases from 180 °C to 220 °C. For example, at 4 m/s the corrosion rate for a carbon steel pipe with an elbow at 180 °C has 14 % higher corrosion rate than the similar pipe at 220 °C as calculated in equation 5.1.

$$FAC\ difference = \frac{1,41E-04\ -1,24E-04}{1,24E-04} = 13,7\ \% \tag{5.1}$$

This is valid when comparing only the flow speeds but in reality, power plants are operated by measuring mass flows. In this case the flow speeds are slightly different even though the mass flow is the same. If we assume that the mass flow needed is 450 kg/s and that the pipe inner diameter is 0,405 m we will end up with the flow speed of 3,92 m/s when the temperature is 180 °C and pressure is 85 bar(a). At 220 °C and at 75 bar(a) the flow speed is 4,14 m/s for the same mass flow. If we calculate the corrosion rates for these flow speed, we will get a real calculated difference for the system components, if the pipe has a same diameter and alloying elements as it typically has on a feed water pipe. At lower temperature

and higher pressure, the corrosion rate is 1,38E-04 mm/y and with higher temperature and lower pressure the corrosion rate is 1,28E-04. In this case the difference is only 7 %.

5.1.3 The point 3, condensate after the low pressure pre-heaters

The point number 3 is located after the low pressure preheaters and before the feed water tank deaerator. The Mihama 3 incident happened in the same place which was one of the reasons to calculate what would be the corrosion rates here with different flow speed and materials. Used fixed values for the figure 5.4 are:

- Pressure 15 bar(a)
- Temperature 150 °C
- pH 9,6
- Iron surface concentration of 4,0E-09 kg/kg
- Diffusivity of 1,5E-08 m²/s
- Metal density of 7800 kg/m³
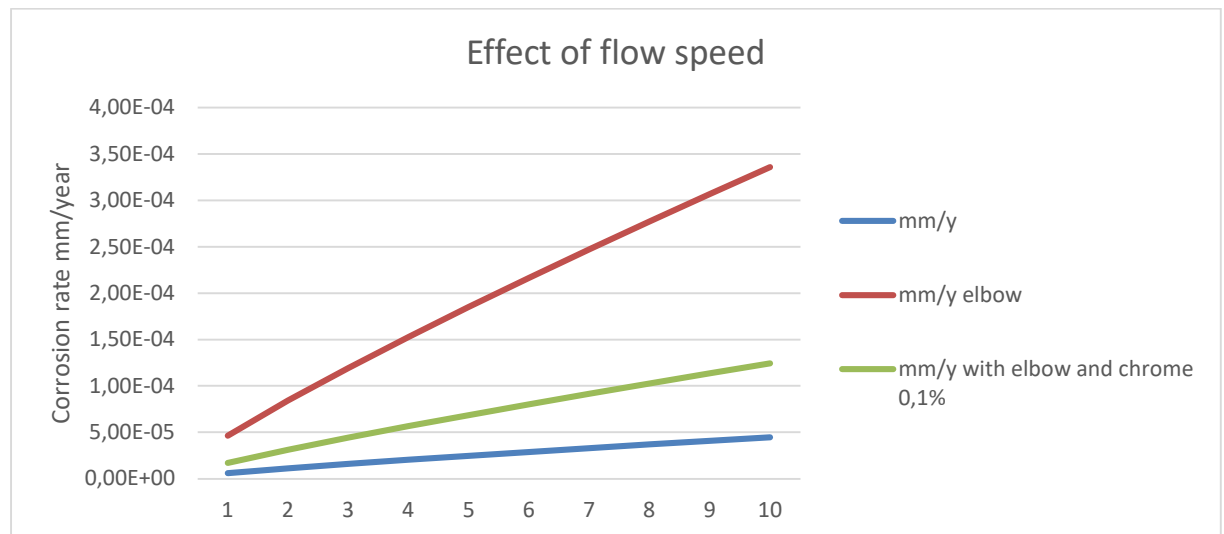
Figure 5.4 Flow speed effect on corrosion rate (pH 9,6 and 150 °C)

The blue line is for straight carbon steel pipe, the red line is for elbow of a carbon steel pipe and the green line is for an elbow of a pipe containing 0,1 % of Chromium. The numerical values are presented in Appendix 2.

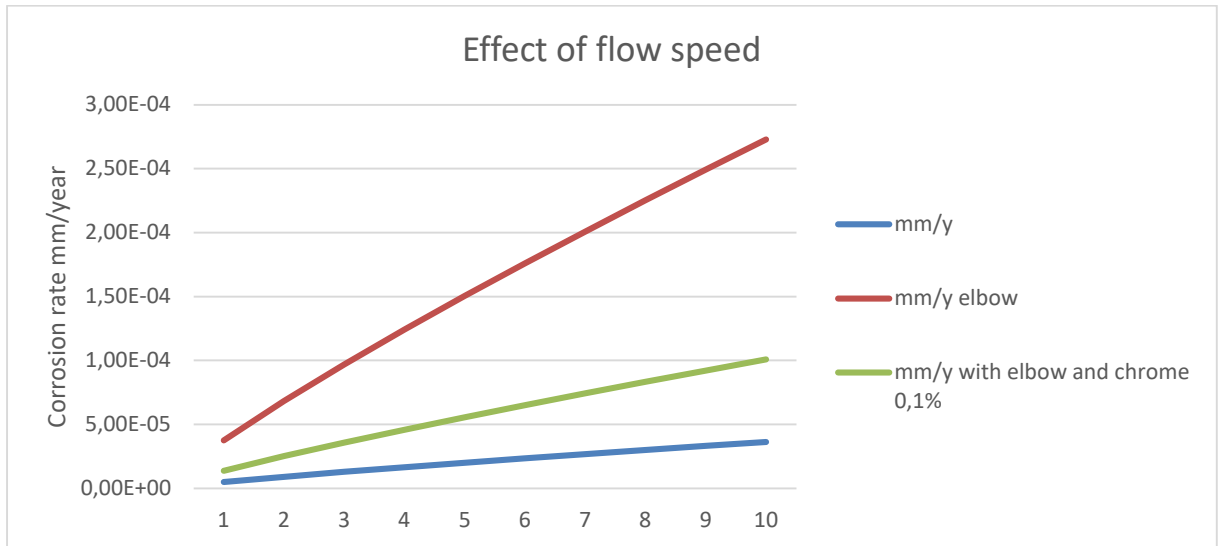As it can be seen from the figure 5.4 the corrosion rates are higher at 150 °C than with the higher temperature. If we compare the same 4 m/s calculated corrosion rate values to the ones calculated for 180 °C and to the 220 °C we can see that the rates are at the highest at

150 °C and decreasing when the temperature increase. The calculated result for flow speed of 4 m/s at 150 °C with an elbow is 1,53E-04 mm/year. This is 23 % more than at 220 °C and 8,5 % more than at 180 °C.

5.1.4   The calculations for carbon steel pipe with different pH values

The figure 5.5 gives corrosion rate for different pH values on a carbons steel pipe. Fixed values in the calculation are:

- Flow speed 6 m/s
- Temperature 150 °C
- Pressure is 85 bar(a)
- Keller coefficient is 10 (tight elbow)
- Carbon steel pipe

Results show a drastic reduction in corrosion rate when pH changes from 7 to 9. Other interesting factor is that when pH is higher than 9,2 the corrosion rate decreases even further before reaching the lowest corrosion rate values. In the figure 3.1 it is shown how the magnetite dissolution rate decrease when pH changes from 7 to 10 and increases when the pH is higher than 11. This has direct impact on how the corrosion rate decreases at pH levels 7-11 as seen in figure 5.5.
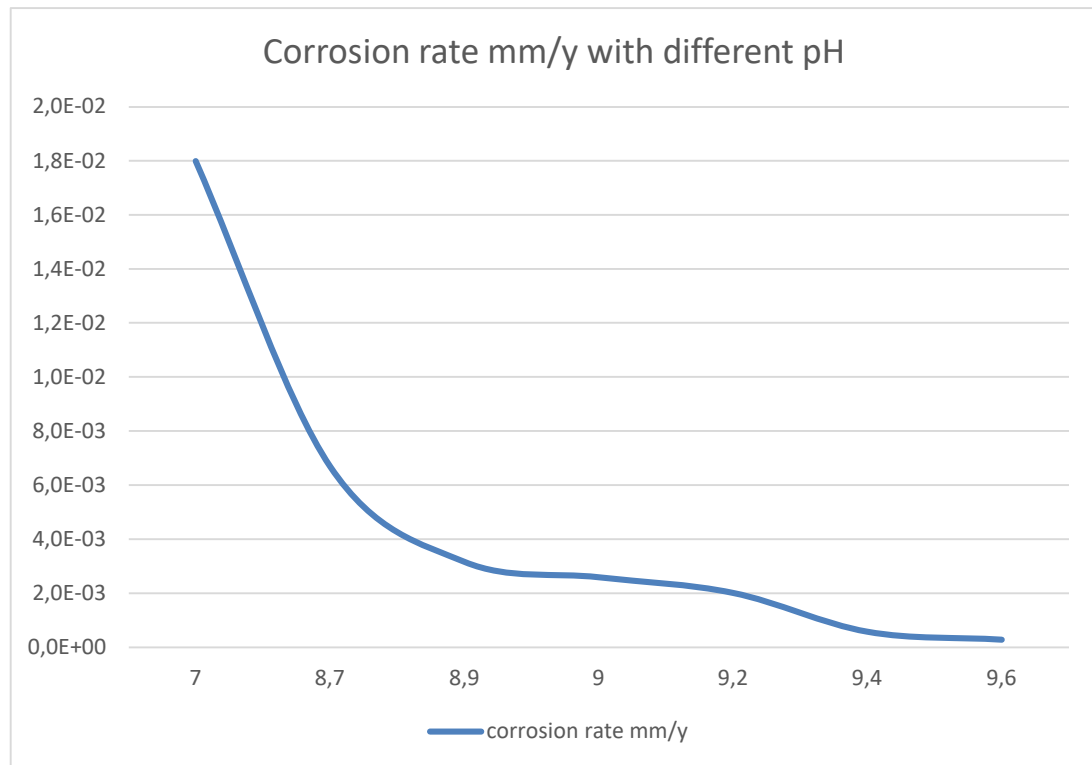
Figure 5.5. The effect of pH on a corrosion rate

Comparing the results at pH 8,7 and at pH 9,6 shows how drastically the corrosion rate change with the pH. The result gives a clear reason why modern pressurized water reactors use high pH values on a secondary circuit. At pH 8,7 the calculated corrosion rate is 6,67E-3 mm/year and at pH level of 9,6 the corrosion rate is 2,88E-04 mm/year. This is almost 96% lower value than at pH 8,7.

5.1.5   The calculations for carbon steel pipe with different temperature values

The figure 5.6 gives corrosion rate for different temperature values on a carbons steel pipe. Fixed values in the calculation are:

- Flow speed 6 m/s
- pH is 9
- Pressure is 85 bar(a)
- Keller coefficient is 10 (tight elbow)
- Carbon steel pipe
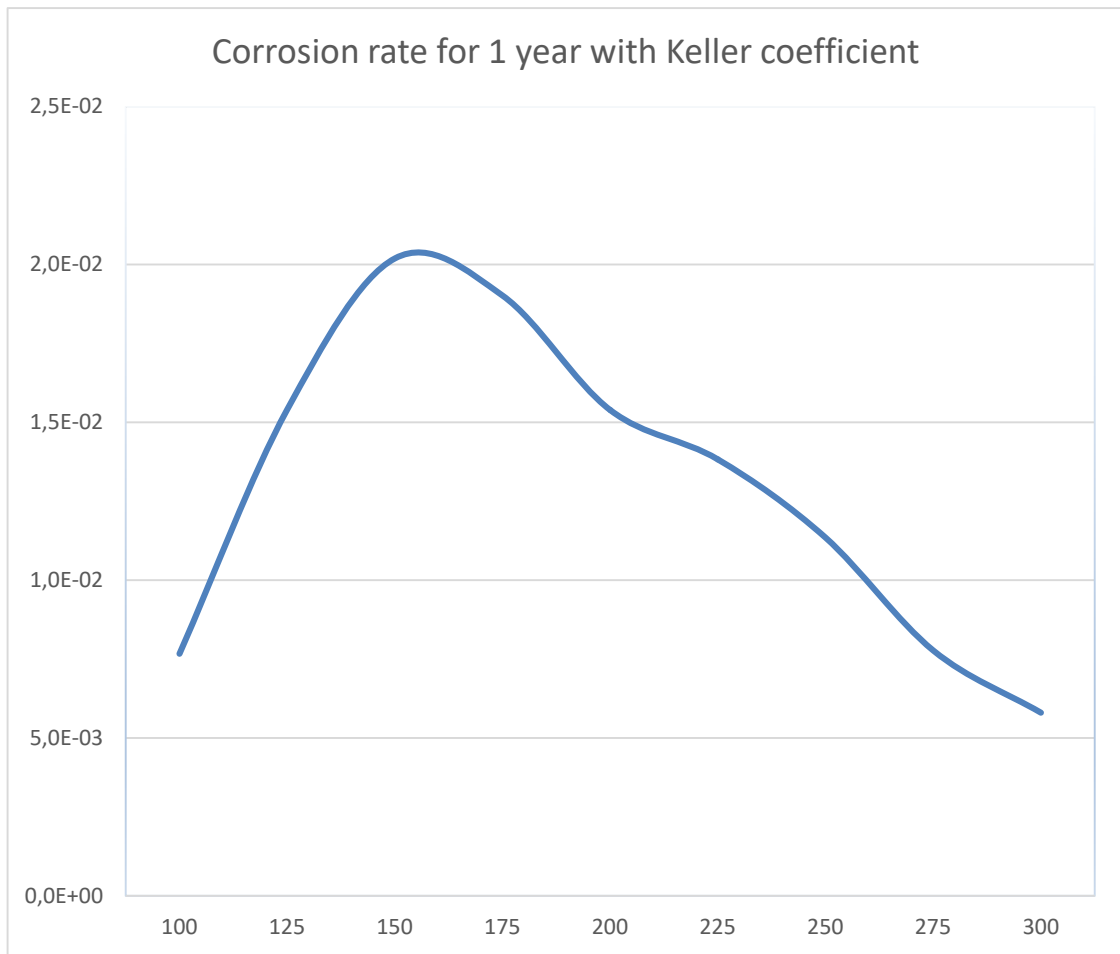
Figure 5.6 The effect of temperature on a corrosion rate

The shape of the curve is what was expected and described in chapter 3.2.2. The calculation confirms the bell-shaped curve having the peak value close to the 150 °C. Reason behind this shape is that when the temperature increases, the diffusivity of the iron soluble species increases. Therefore, the FAC rate should increase when the temperature is increasing but at the same time the iron oxide solubility decreases at temperature higher than 150 °C. The Iron oxide solubility is heavily influenced by pH and temperature as can be seen from figure 4.1. Both variables increases until temperature is 150 °C. Then the solubility will start to decrease. This can be confirmed in the calculation results in Appendix 3.

5.2   Two-phase flow calculation

For the two-phase flow calculation 3 typical location for flow accelerated corrosion are chosen based on the temperature and moisture content. It's well known that the dry steam piping does not suffer from flow accelerated corrosion as for example the live steam pipes

from the steam generator that has a really low moisture content. In nuclear power plant basically all other steam pipes have some moisture and therefore are prone for corrosion. This is because the steam used is in saturated state and therefore any energy taken out from it will increase the moisture content of the steam. The only location where the steam is super heated is after the moisture separator re-heaters but it's typically for a short distance from the heater to the turbine.

5.2.1   The point 4, steam line to high-pressure pre-heaters

The point number 4 in figure 5.1 is a steam extraction line to the high-pressure pre-heaters. At this point the moisture content is already quite a significant and the temperature is typically a bit above 200 °C. The used fixed values for the point number 4 calculation are:

- Pressure is 23 bar(a)
- Temperature 220 °C (saturation temperature for 23 bar(a))
- Keller coefficient for straight pipe Kcs = 0,04
- Keller coefficient for elbow Kc = 0,3
- Temperature coefficient f(T) = 0,16
- Steam fraction x = 0,9

Calculation results are shown in figure 5.7. The blue line is for straight carbon steel pipe, the red line is for elbow of a carbon steel pipe and the green line is for an elbow of a pipe containing 0,1 % of Chromium. The numerical values are attached to the Appendix 3. The result shows that the corrosion rate increases linearly with the flow speed. Other interesting point is that the corrosion rates are significantly higher than in one-phase flows. This is caused by much higher flow speeds used in the steam pipe lines. Let's see what are the results in other location where the moisture content is higher and the temperature is lower.
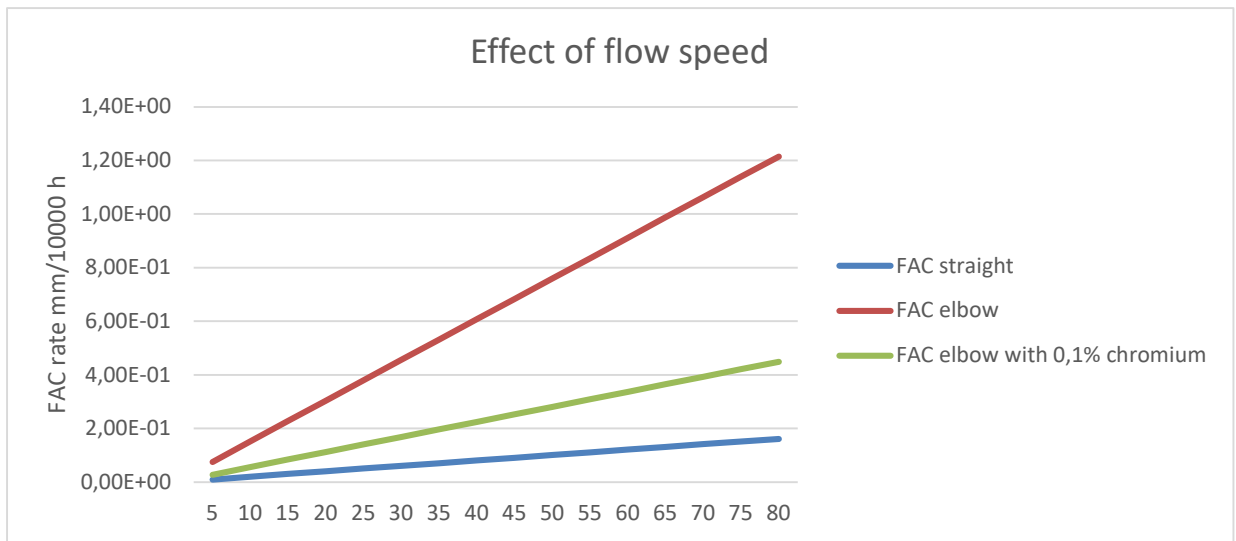
Figure 5.7 Corrosion rates at steam fraction of 0,9 and temperature 220 °C

5.2.2 The point 5, steam line to the moisture separator re-heater

The point number 5 in figure 5.1 is the steam extraction line after the high-pressure turbine to the moisture separator re-heater. Function of the MSR is to first separate the moisture from steam and then reheat the dried extraction steam with the live steam, or in case it's a two-phase heating, with a live steam and steam from one of the turbine extraction lines. This is where the moisture content is typically at the highest level on a secondary circuit side, except the low-pressure turbine extraction lines where the temperature is typically low and is not considered as a potential area for FAC to occur. The fixed values used for point number 5 calculation are:

- Pressure is 10 bar(a)
- Temperature 180 °C (saturation temperature for 10 bar(a))
- Keller coefficient for straight pipe $K_{cs} = 0,04$
- Keller coefficient for elbow $K_c = 0,3$
- Temperature coefficient $f(T) = 0,45$
- Steam fraction $x = 0,85$

Calculation results are shown in figure 5.8. The blue line is for straight carbon steel pipe, the red line is for elbow of a carbon steel pipe and the green line is for an elbow of a pipe containing 0,1 % of Chromium. The numerical values are attached to the Appendix 4.

Results show significant increase in corrosion rate compared to the ones calculated for high pressure pre-heaters, which was expectable since the temperature coefficient used in the calculation is at the highest point and the moisture content is 5 % higher. If we compare the results from the points 4 and 5 at the typical saturated steam flow speed of 35 m/s we can see that the point number 5 have 3,5 times higher corrosion rates as was calculated for point number 4.

Effect of flow speed

FAC rate mm/10000 h

- FAC straight
- FAC elbow
- FAC elbow with 0,1% chromium
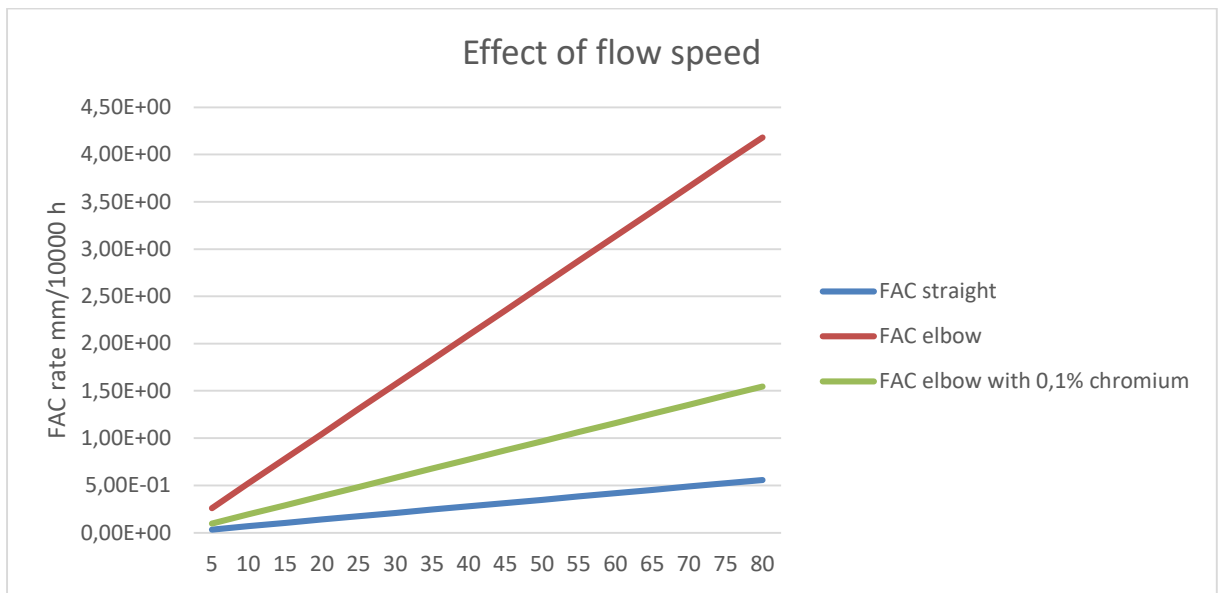
Figure 5.8 Corrosion rates at steam fraction of 0,85 and temperature 180 °C

5.2.3 The point 6, flash steam pipe

The point number 6 in figure 5.1 is a bit exceptional compared to the points 4 and 5 since the drain lines are typically designed for saturated water. Problem with the saturated water is that if there is any pressure reduction in the system, the water will evaporate. This happens typically in a system where the saturated condensate is collected in tank and pumped back to the process. The flashing of the condensate happens if the pressure in the connected tank is lower than in the tank where the condensate is collected. Bigger the pressure difference there is, bigger amount of water will evaporate. Since the steam density is much lower than the water density, the flow speed will increase significantly. For example, if saturated water at 15 bar(a) is pumped into the tank that has a pressure of a 10 bar(a), the amount of flash steam is 4 %. This might seem like a small amount but since the saturated steam at 10 bar(a) has 172 times lower density than the saturated water at 10 bar(a), it will increase the flow speed 7-fold compared to the saturated water. If this is not considered in pipe sizing, the flow

speeds can be really high and can cause even erosion in the pipe. Erosion is not considered in the calculation but it has significant impact on a pipe lifetime and should be considered when choosing materials and sizes for pipes carrying saturated water. So, based on this, what would be the corrosion rates for two-phase flow carrying only 4 % of steam?

Figure 5.9 shows the calculation results for the two-phase flow of 4 % steam content. Fixed values for this calculation are:

- Pressure is 10 bar(a)
- Temperature 180 °C (saturation temperature for 10 bar(a))
- Keller coefficient for straight pipe Kcs = 0,04
- Keller coefficient for elbow Kc = 0,3
- Temperature coefficient f(T) = 0,45
- Steam fraction x = 0,04

Once again, the blue line is for straight carbon steel pipe, the red line is for elbow of a carbon steel pipe and the green line is for an elbow of a pipe containing 0,1 % of Chromium. The numerical values are attached to the Appendix 4.

If results are compared to the point number 5 with same steam pressure and temperature parameters, we can see that the calculated corrosion rates are more than 50 % bigger with very low steam content.
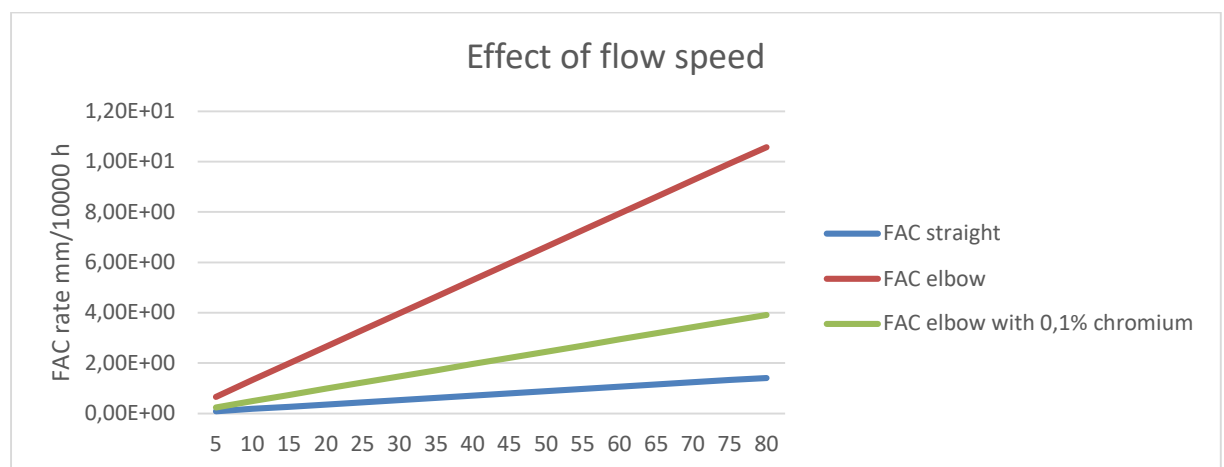
Figure 5.9 Corrosion rates at steam fraction of 0,04 and temperature 180 °C

5.2.4 The calculation for different moisture contents

Based on the calculation done for the two-phase flows it's clear that the moisture content is one of the biggest contributors to the FAC phenomena. But how big of an impact the moisture content has? This is calculated in figure 5.10. Fixed values for this calculation are:

- Pressure is 10 bar(a)
- Temperature 180 °C (saturation temperature for 10 bar(a))
- Keller coefficient for straight pipe Kcs = 0,04
- Keller coefficient for elbow Kc = 0,3
- Temperature coefficient f(T) = 0,45
- Flow speed v = 20 m/s

As before the blue line is for straight carbon steel pipe, the red line is for elbow of a carbon steel pipe and the green line is for an elbow of a pipe containing 0,1 % of Chromium. The numerical values are attached to the Appendix 5. From the figure we see that the corrosion rate does not increase linearly with the moisture content. At the low moisture contents the corrosion rates increase more than it does at higher moisture contents. For example, the corrosion rate increases 42 % when steam content decreases from 98 % to 96 % but only 5 % when the steam content decreases from 80 % to the 78%.
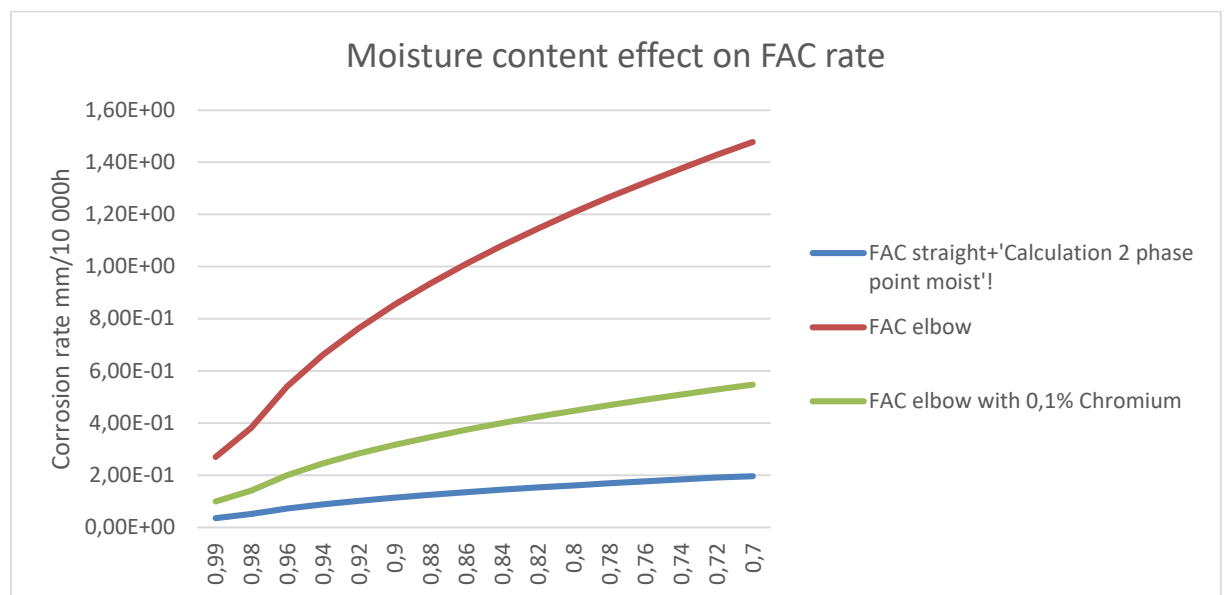
Figure 5.10 Corrosion rates at different moisture contents

5.3   Results

Results for both the single- and two-phase flows seem to be in line with the literature. The corrosion rate increases when the flow speed is increased, and the chromium will decrease it. The FAC is at the highest between 150 and 180 °C and that the pH has significant impact on the corrosion rate. The elbows and other flow restrictors will create turbulency and enhance the FAC rate as do the moisture content.

The basics of the FAC are correct but how about the actual numerical values. How do we know if the results are correct? In Chapter 6 the results from the developed tool are compared with the results from the other studies and the future research topics are given.

6   DISCUSSION

So far the corrosion rates for several locations with different parameters are calculated but how reliable those results are? This chapter examine couple of examples from other studies and calculate corrosion rate with our own equations. One study for one-phase flow calculation and one study for two-phase flow calculation are used for the purpose. Later in the chapter, we will discuss how well the results are corresponding and from where the differences in the result might come from. We have recognized from all the reports we have used in the thesis that the importance of correction factors seems to be significant, and we do not assume to have exactly same values but perhaps we can point out the differences and even spot a pattern.

After comparison the results are analyzed objectively, and the reliability of the study is examined. At the end of the chapter the key finding are listed and the topics for the further research defined.

6.1   Comparison of results to other studies

The single-phase corrosion study to be compared is taken from Japan Society of Maintenology E-Journal written by S. Uchida. Calculation method is a similar to our way of estimating the corrosion rate but in their study, they have used computational flow dynamics to get more precise information about the turbulency and the flow patterns in the pipes. They also had real measured thinning rates from existing nuclear power plants that they have used in their calculations.

The two-phase flow calculation study is from Russian article on corrosion rates in the nuclear power plants written by Baranenko V. I. This study is based on Russian software called ЭКИ-03. The paper contains initial FAC rate calculation results, as well as information for measurements made during operation. The study also defines process parameters so that we can calculate our own estimates and compare how well they correspond to the calculated and measured rates in the paper described above.

6.1.1   Comparing single-phase flow calculation

In the S. Uchida study, the corrosion rate is calculated by using mass transfer coefficient for a straight pipe. This result is then multiplied by the geometrical factor for other geometries. This is the same principle as we have used in the calculation. They have also used the computational flow dynamic software to get a more precise flow parameters for their calculations. This of course would be beneficial in existing plants so that the real flow parameters could be used. We just use the same values as they have done so we should not have differences in the flow dynamics. All the steps performed in referred paper are shown in figure 6.1. The important thing to note is that they have made some modification to the calculation code based on the measurement data. These changes are not explained but assumably some other correlation factors have been used to get the results closer the actual measured data.
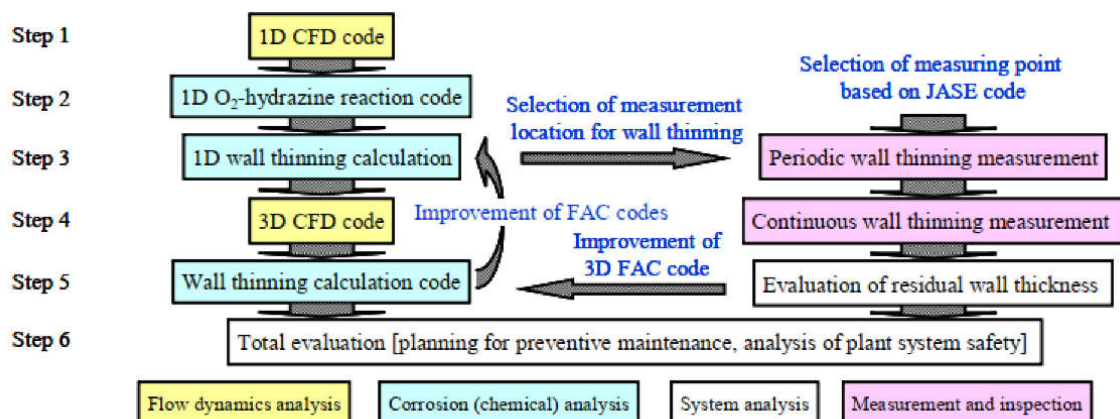
Figure 6.1 Calculation steps in S. Uchida study

Since we do not have access to the data they have used, we have to rely on calculation code alone. This part in the Uchida study is shown in figure 6.2. The input parameters shown in figure 6.2 are mostly the same what we have used. Materials, temperature, flow velocity distributions, pH, oxygen concentration and geometry factors. These are the steps 1 to 3 in figure 6.1.
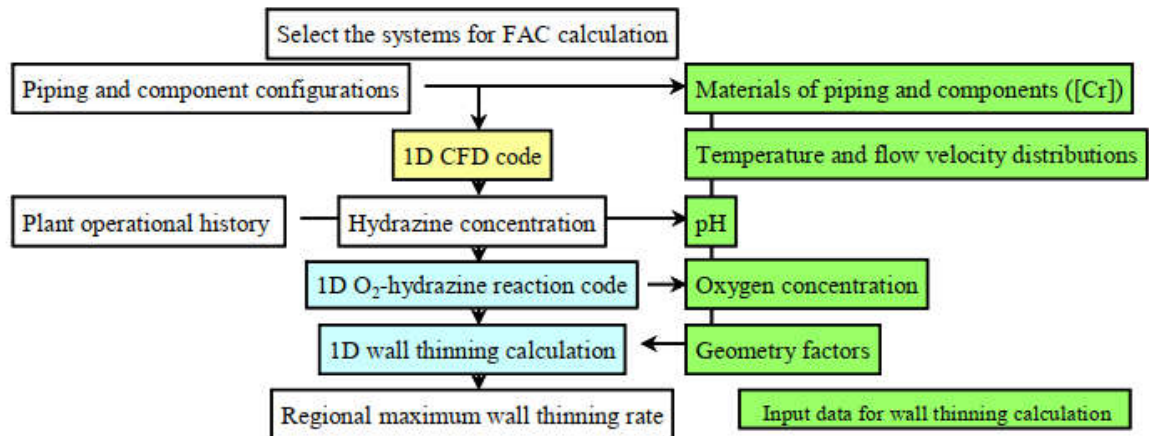
Figure 6.2 1D calculation steps and parameters used / *S. Uchida/*

The only parameters we have not used in our calculation is the oxygen concentration but since in a typical pressurized water reactor power plant the oxygen content is kept on a low level in the secondary circuit, the effect of it should be minimal. They have estimated corrosion rates in 16 different locations with different parameters. The fixed values they have used are chromium content which is 0,01 w% and can be left out of calculation due to lower level than the 0,04% threshold value as explained in chapter 3.2.4. They have used correction factor of 0,99 so the effect of Chromium at 0,01 w% is 1 % for the corrosion rate. The pH value is expected to be 9,2 for all the locations. The oxygen concentration is 0 ppb and ferrous ion concentration (Fe^{2+}) in the bulk water is expected to be 0 ppb. The maximum Mass Transfer Coefficient is calculated by multiplying the Mass Transfer Coefficient with the Keller coefficient. This is calculated same way as we have by dividing the Geometrical factor with a straight pipe factor (0,04).

Let's take their calculation into closer examination. These location numbers are defined in the reports chapter 3.2.5. They are located in a different part of the secondary circuit and all have the same fixed values listed before and the ones that are changing are listed in table 6.1. We will use the same values in our own estimation.

Table 6.1 Parameters used in the report and the corrosion rates (Uchida 2013, p. 108.)

Location	Pipe inner diamt. (m)	Flow velocity (m/s)	Temp. (°C)	Pressure (MPa)	Geometrical factor K_c	Mass transfer coefficient (m/s)	Max. Mass transfer coefficient (m/s)	Corrosion rate mm/year
1	0,620	3,58	33	2,64	0,16	1,5E-04	6,02E-4	0,05
2	0,381	3,16	33	2,62	0,23	1,5E-04	8,64E-4	0,07
3	0,381	3,23	74	2,35	0,23	3,18E-4	1,83E-3	0,25
4	0,425	2,59	74	2,38	0,23	2.61E-4	1,5E-3	0,21
5	0,425	2,63	98	2,04	0,23	3.57E-4	2,05E-3	0,32
6	0,425	2,7	129	1,71	0,15	5.00E-4	1,87E-3	0,27
7	0,425	2,75	146	1,41	0,15	5.87E-4	2,2E-03	0,27
8	0,687	3,15	146	1,39	0,5	5.96E-4	7,45E-3	0,93
9	0,437	3,68	178,9	0,97	0,16	9.45E-4	3,78E-3	0,28
10	0,384	4,17	186	3,22	0,15	1.13E-3	4,22E-3	0,27
11	0,519	4,49	186	3,19	0,3	1.12E-3	8,44E-3	0,53
12	0,483	5,19	188	7,21	0,3	1.30E-3	9,73E-3	0,59
13	0,483	5,19	188	7,12	0,3	1.30E-3	9,73E-3	0,59
14	0,483	5,44	222	7,01	0,3	1.66E-3	1,24E-2	0,29
15	0,701	5,16	222	7,01	0,6	1.47E-3	2,2E-2	0,52
16	0,354	5,06	222	7,04	0,3	1.66E-0	1,25E-2	0,30

With the parameters in table 6.1 and with the fixed value they have calculated the corrosion rate shown in the last right column.

So how close do we get with our calculations? The results can be seen in the table 6.2. It contains not only the corrosion rate but also Reynolds number, Schmidt number and Sherwood number. We haven't calculated all the location since many of them are for similar conditions. So, we have selected the ones which differ most from each other.

Table 6.2 Corrosion rates calculated

Location	Reynolds number	Schmidt number	Sherwood number	Keller coefficient	Corrosion rate with keller coefficient mm/year
1	2,960E+06	2,687E+02	3,841E+04	4,0	0,000025
4	2,81E+06	6,553E+01	2,3E+04	5,75	0,00006
7	5,73E+06	1,455E+01	2,590E+04	3,75	0,00039
12	1,535E+07	8,595E+00	5,709E+04	7,5	0,0012
14	1,828E+07	5,748E+00	5,170E+04	7,5	0,0011

Based on the results, the calculated values are a lot smaller than the ones calculated in the report. On a figure 6.3 the results are shown in a logarithmic scale. There we can see that the trend is similar in both the calculated and in the values given in the report. The difference is bigger at the lower temperatures and at the lower mass transfer coefficient values. To be noted that even at higher temperature and at higher mass transfer coefficient values, the calculated corrosion rates are several hundred times smaller than in the report.
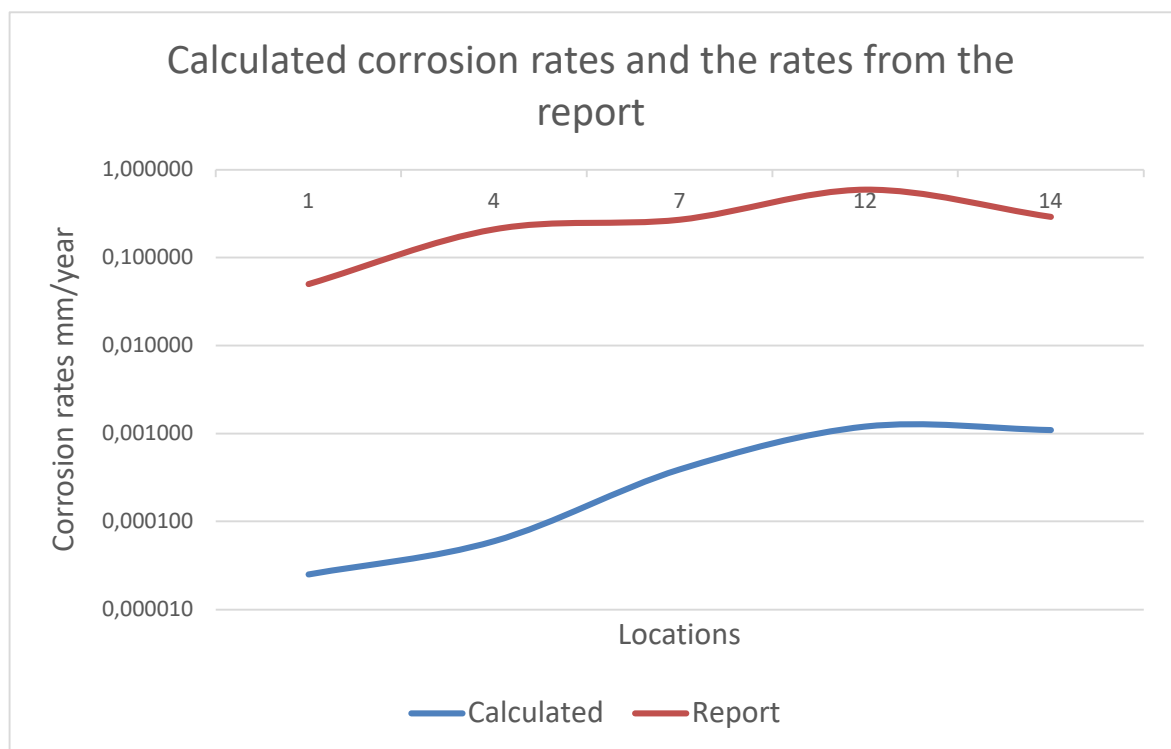
Figure 6.3 Comparison of calculated corrosion rates to the report on logarithmic scale

The difference is significant, especially when considering that many of the inputs for the calculation are physical properties and should be same in both cases. So where the difference

is coming from? One possibility is the Sherwood number. We have calculated it as shown in the equation 6.1. Also given in Chapter 4, equation 4.4.

$$Sh = 0,0165 \cdot Re^{0,86} \cdot Sc^{0,33} \qquad (6.1)$$

In the report they have calculated it a bit differently. There they have used formula shown in equation 6.2 where **d** is the pipe inner diameter (m).

$$Sh = \frac{0,23}{d \cdot Re^{0,8} \cdot Sc^{0,33}} \qquad (6.2)$$

Other changes are that they have added pipe diameter to the calculation and used different multipliers. Reynolds number can be calculated only one way and the Schmidt number is based on diffusivity and kinematic viscosity. Both are physical properties as explained in chapter 4. Therefore, we can calculate how big of an impact it would have to the Sherwood number with the equation they have used. The results are shown in table 6.3 where the Sherwood number on a left column is the one calculated with equation 6.1 and the right one is with the equation 6.2.

Table 6.3 Comparison of the Sherwood numbers

Location	Sherwood number	Sherwood with equation in report	Difference in %
1	3,84E+04	3,532E+04	109
4	2,30E+04	3,095E+04	74
7	2,59E+04	3,339E+04	78
12	5,71E+04	5,431E+04	105
14	5,17E+04	5,471E+04	94

Interesting about the difference in the Sherwood number is that the difference is not equal for all the cases. The location 12 is almost the same as the one we have calculated and then at the location 4 the difference is 26 %. If the difference would be only based on the added diameter into the equation, the difference should be the same but since the equation is modified fully, the difference changes based on the diameter, Reynold number and Schmidt number. Most likely they have used this equation because it fit's better for these process parameters. On the other hand, so should the equation we used. In Chapter 4 it was explained

that this equation is valid for Reynold number from 10^4 to 10^7 and as we can see from table 6.2 we are well withing this range.

If we now calculate corrosion rates again with the new Sherwood number, do we get any closer to the ones in the report? The figure 6.4 shows the results. The blue line is the corrosion rates calculated with the Sherwood number from equation 6.1 and the green one is the corrosion rates calculated with equation 6.2.
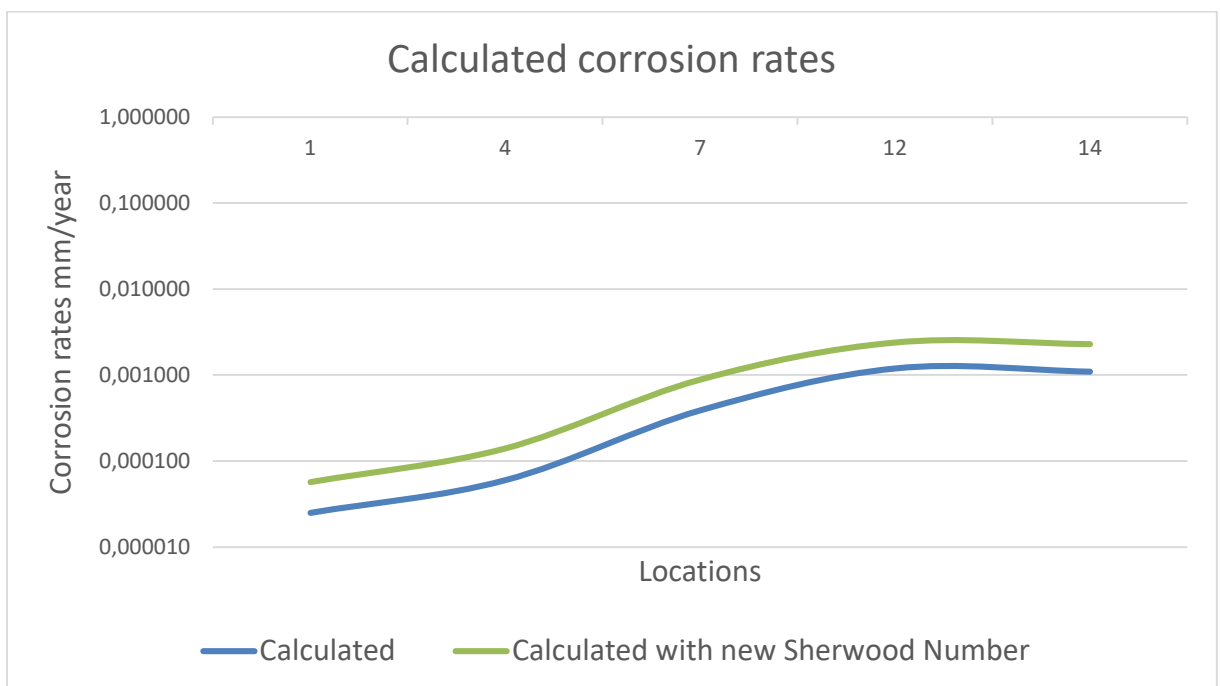
Figure 6.4 Comparison of the Sherwood numbers impact for the calculation

The corrosion rates are closer to the values calculated in the report but still the difference is significant. In the report the calculated corrosion rates are tenths of a millimeter and we calculate thousands of a millimeter. Therefore, this cannot be the cause for the differences.

It seems that results are closer to the reported corrosion values when the flow speed, pressure and the temperature increases. The flow speed affects the Reynolds number, that affects the Sherwood number so the impact from it is small as tested earlier. The temperature has a bigger impact since it affects both the iron ion concentration at the boundary layer of oxide layer and the flowing water and the diffusivity through the oxide layer. Since these are all physical properties the difference must come from the correction factors that are not given in the report. And since the difference is not equal in all the location, they have used different

correction factors for each location. Most likely this is related to the temperature and perhaps to the pipe size. The pipe size could affect the flow accelerated corrosion rate in a similar way as the pressure losses in a pipe is smaller when the pipe size is larger even though the flow speed is the same. This is because the pressure loss is due to the turbulence created by the surface roughness of the pipe. This turbulence affects a bigger cross area in a smaller pipe than in a larger one, therefore the bigger pipe can have bigger flow speed with same pressure loss. This pressure loss and the turbulence caused by it is the driving force of a flow accelerated corrosion in a pipe and therefore the corrosion rates might differ just because of the pipe diameter even when the other parameters would be same.

6.1.2 Comparison of two-phase flow calculation

For the two-phase flow calculations verification, Russian article on corrosion rates in the nuclear power plants written by Baranenko V. I. is found to be suitable for the purpose. All the tables used as an input are taken from the referred study. There the corrosion rates for two-phase flow are calculated by ЭКИ-03 software. The purpose of the study is to present Russian software, which to be used for estimation of FAC rate in Russian VVER NPPs. Typically, the flow accelerated corrosion rates are considered to be linear over time but in reality, the corrosion rate is larger at the start of the operations and reduces over time when the protective magnetite film is formed. Presented software gives possibility to calculate FAC rates in the beginning of pipeline operation, in the end of the pipeline lifetime as well as for specific period.

In the paper used for verification, FAC rate calculation in ЭКИ-03 software is based on:

$$W_{FAC} = C_0 * F_1(T) * F_2(XC) * F_3(v) * F_4(O_2) * F_5(pH) * F_6(K_k) * F_7(\alpha) * F_8(A) * F_9(\tau)$$

where:

W_{FAC} – corrosion rate, mm/year

C_0 – coefficient equal to 1 mm/year

$F_1(T)$ – coefficient considering temperature

$F_2(XC)$ - coefficient considering steel content

$F_3(v)$ – coefficient considering flow rate

$F_4(O_2)$ – coefficient considering Oxygen concentration

$F_5(pH)$ – coefficient considering pH

$F_6(K_k)$ – coefficient considering geometry (Keller coefficient)

$F_7(\alpha)$ – coefficient considering water content in steam (for one phase flow $F_7(\alpha) = 1$)

$F_8(A)$ – coefficient considering using of additives (NH_4, ethanolamine, etc.)

$F_9(\tau)$ - coefficient considering operation time

Based on FAC rate estimation made by ЭКИ-03 software, conclusion is made that the most critical factors having effect on FAC rate in NPPs are the low or zero Chromium content in the steels, complicated pipeline geometry, poor design and wrong materials selection. One of the most damaged section in the pipelines because of FAC are the areas before and after welded joints. (Baranenko et al. 2013, p. 1-14.)

The input parameters they have used for the calculation are shown in table 6.4. The point number 1 describes that this is for steam, the point 2 define the amine used. Based on chapter 3.2.1 this factor should not have a big influence on the calculated corrosion rate. The point 3 is the temperature in °C and it has a big impact on a corrosion rate as described in chapter 4. The point 4 is the steam pressure and since we are now talking about the moist steam, it should correspond to the temperature in point 3. The point 5 is the pipe outer diameter and point 6 is the wall thickness, both in meters. These are used to calculate the flow speed. The point 7 is the Keller coefficient. Points 8, 9 and 10 are Chromium, Molybdenum and Copper contents in %, but since they are present at such a small quantity, below the threshold value to reduce the flow accelerated corrosion rate, they can be left out from our calculations. The point 11 is the start time in year, in this case 0 and the point 12 is the end time in years. The point number 13 is the time between points 11 and 12, in other words, time to flow accelerated corrosion to develop. The point 14 is the steam flow amount in tons/hour. Point 16 is the steam-water mixture rate in mm/year. Point 17 is the moisture content in %. The point 18 is the water speed m/s. The point 19 is oxygen content in steam in µg/kg and the point 20 is the pH. The point 21 is the FAC rate at the beginning, 22 is the FAC rate at the end and 23 is the average FAC over the time period in mm/year. The point 24 is the wall thickening for the period in mm.

Table 6.4 Inputs used for the calculation two-phase flow calculation (Baranenko et al. 2013, p. 1-14.)

№	Наименование	Размерность	Значение
1	Теплоноситель - пар	-	-
2	Амин - режим бескоррекционный	-	-
3	Температура пара, °С	°С	200
4	Давление пара,	МПа	0,16
5	Наружный диаметр	м	630
6	Толщина стенки	мм	12,0
7	Коэффециент Келлера	-	0,6
8	Концентрация хрома	%	0,03
9	Концентрация молибдена	%	0,03
10	Концентрация меди	%	0,03
11	Время начала расчета ЭКИ	лет	0,0
12	Время конца расчета ЭКИ	лет	17,6
13	Полное время расчета ЭКИ	лет	17,6
14	Расход пара	т/час	445,0
16	Скорость пароводяной смеси,	мм/год	51,8
17	Коэффициент влажности	%	5,0
18	Скорость циркуляции воды	м/сек	0,49
19	Концентрация кислорода в паре	мкг/кг	4,0
20	Водородный показатель pH	-	8,2
21	ЭКИ в начале расчета	мм/год	2,72
22	ЭКИ в конце расчета	мм/год	0,5
23	Среднее ЭКИ за расчетное время	мм/год	0,68
24	Утонение за расчетное время	мм	12,0

Based on this we can calculate and compare how close we will get to the reported values. In our calculation we use only the pressure, temperature, mass flow, steam fraction, pipe outer diameter, wall thickness and Keller coefficient. (Baranenko et al. 2013, p. 1-14.)

With these values we will get 2,9 mm/10000h and if we assume that the year have a 8760 operating hours, the corresponding corrosion rate would be 2,6 mm/year. This is close to the value in the report for the corrosion rate in the beginning of the operation. Problem with this result is that at the end of the operating period the corrosion rate is only 0,5 mm/year and that the average corrosion rate for 17,6 year is 0,68 mm/year. Based on the average corrosion rate we can estimate that the higher corrosion rate takes place only at the beginning of the operation and then the corrosion rate stays stable. This is due to the missing protective oxide layer on beginning of operation. The magnetite layer forms on a steel surface during the first year of operation and then reduces the corrosion rate to the nominal level. In this case the

level is 0,5 mm/year. In this case, the pipe would corrode 7,2 mm in a 10-year period. That's more than half of the original 12 mm thickness and would cause parts of the pipes to be replaced causing additional downtime for the plant. This should be considered when choosing the pipe materials, especially if the pipe is located in a place where the maintenance or replacement is difficult and time consuming. Typically, these locations are designed to last for the plant operation lifetime, or at least the 30-year operation time as in many conventional power plants.

The equation for calculation of FAC rate in two-phase flow does not contain the factor for pH. If it would be taken into account, the results might be closer to the values given in the EKI software. We could add a pH coefficient into the calculation from figure 4.1. The corrosion rate is now calculated for pH-7 and in this example the pH is 8.2, the coefficient could be calculated by dividing the iron concentration at pH 8,2 and 200 °C with iron concentration at pH 7 at 200 °C and multiply this with the calculated corrosion rate. In this case it would be $\frac{120 \ \mu g/kg}{180 \ \mu g/kg} = 0{,}67$. Then the calculated rate of 2.6 mm/year is multiplied with the pH coefficient, the result is 1,7 mm/year. This is still three times the corrosion rate calculated with EKI software. Direction is correct but the impact of it is not enough. Of course, these kinds of coefficients should be based on test and real measured data instead of by creating own multipliers to the equation. It's clear that the pH has a significant impact on corrosion rate, it should also be added into the equation and since we don't have the data available that the commercial flow accelerated corrosion calculation software has, it is very difficult to define correct coefficient for the pH that should also be based on the measured data.

6.1.3 Comparison outcome

Comparison of the results shows that there are big differences in the results and that the difference is not linear in single phase flow situation. The method of calculation is the same in both the tool and in the referred study. For example, the Sherwood number formula is a bit different than in the calculation tool, but it has only a small impact on the results. More importantly, the difference between results is equal in all cases as can be seen from figure 6.4. The outcome of this is that the input from the test have a significant impact on corrosion rates calculation and that coefficient should be added on the tool developed for this thesis.

The two-phase flow calculation tool gives correct corrosion rates for the first year of the operation when the protective oxide film is not formed yet. This is due to the fact that our tool calculates the corrosion rate for neutral pH level and in the reference study the pH used is 8.2. If the pH would be the same, most likely the results would differ more than they do now.

What was not considered in our calculation is the effect of erosion-corrosion. This can be a significant factor when calculating the FAC rate and as we can see from the results, the coefficient used based on the real measured data plays a key role. Assumption is that the coefficients used contain partly factors from the erosion-corrosion. This would explain the non-linear difference in the results.

6.2   Objectivity of the study

The objectivity of the study can be measured by considering what kind of methods is used and how well those can be justified. This is considered when creating the calculation tool and when reporting the results in chapters 4 and 5. For the developed tool the equations used are taken from the literature and the inputs are based on the physical properties. Therefore, the results can be considered reliable basis for the further development.

Comparison in chapter 6.1 shows that even the trend of the corrosion rates are similar in the developed tool and in the reference study, the actual corrosion rates differ from each other's. These differences are considered in chapter 6.1 and the possible reasons are defined. The parameters not considered in the tools are the ones that can not be found from the literature but are based on the measured data. From this measured data, the correction factors have been added to the equations in the reference studies. These correction factors are the know-how of the existing FAC calculation tools as described in the chapter 3.3.

6.3   Reliability of the study

The reliability of the study can be estimated on two ways. First one is the references. How the information given the study can be justified and is it possible for others to replicate the study and the results. Since the equation used are from the literature and valid for the NPP secondary circuit flow parameters, the result should be reliable. The parameters used for the calculation are also based on the literature values so replicating the calculation should be possible.

The second method of reliability analyze is the comparison of the results with other studies as done in the chapter 6.1. Considering this the calculation tool results are not exactly correct, but neither is the existing calculation tools. They update their functions as more data from the existing plants and research programs is available.

Since the trend of the results is the same in developed tool as in the referred studies, the assumption is that the basis are correct but the numerical values should not be considered as real future corrosion rate but as an estimation of the location where the FAC might occur.

6.4 Key findings

The key findings of the study are that the corrosion rate is affected by a several different factors as explained in the chapter 3. These individual factors are commonly known but what was found out during this study is that the information how other factors influence on others is not well known. This is the reason why the existing calculation tools rely on the measured data and correction coefficients.

The actual corrosion rate most likely will differ from the calculated rate and that the difference might not be equal when estimating corrosion rates with different parameters. Therefore, the results should be compared with the similar kind of process parameters and then choose the locations to be inspected. This might be the most practical way of using the developed tool.

6.5 Research novelty value and practicality

The research novelty value comes from the results of the calculation done in the chapter 4 and 5. What is interesting to see is the similarities in all the referred calculation tools and in the developed tool for this study. Equally interesting is the fact that the flow accelerated corrosion is not yet well-known phenomena and there are no universal equation to be used for all the situation. Instead, the commercially available tools rely on correction factors based on measured data. This shows that the correlation factor used for one situation does not apply for other location with different process parameters.

One of the main targets of the Thesis was to develop a practical tool to be used for estimating corrosion rates with different parameters. In the chapter 6.1 the results of the developed tool

is compared to the other studies done with different FAC calculation tool. The results show that the developed tool makes it possible to define locations that are more prone to the FAC but the actual corrosion rate calculated is optimistic when comparing results to the referred study. For the two-phase flows the situation is better when it comes to the referred results and the tool gives higher corrosion rates than in the reference study.

The practicality of the tool can be shown also when considering future operating years. Let's take the two-phase flow calculation as an example.

The calculated corrosion rate would decrease the wall thickness of the steam pipe into half just under 10 years. This would cause some replacements works in every 10 years. What about if there's a chance to change materials before the actual pipe is designed or installed? What should be the Chromium content be to reduce the corrosion rate to 6 mm for the 30 year period. This can be seen from figure 6.5. The basic assumption has been that the corrosion rate would be 0,5 mm/year and 15 mm for 30-years.
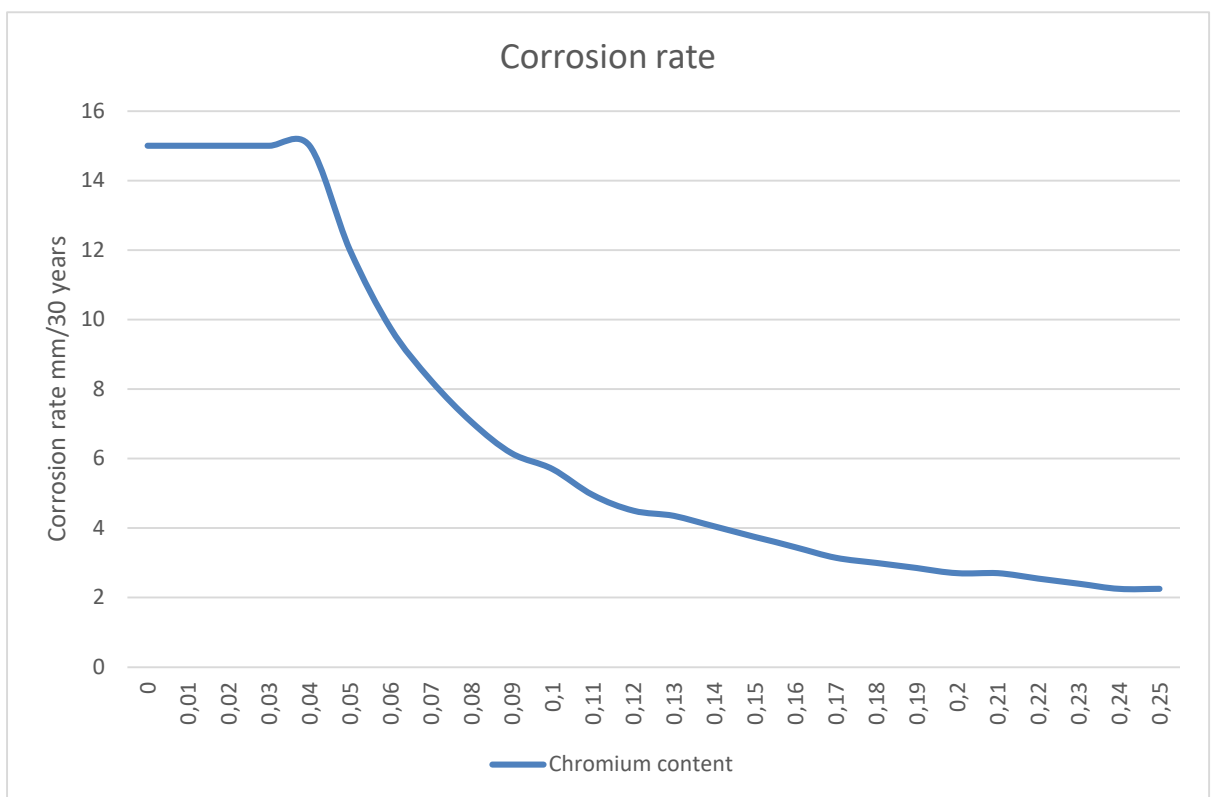

Figure 6.5 Chromium effect on corrosion rate.

From the figure 6.5 we can see the needed chromium content is 0,1%. With this small change in the material there is a chance to reduce the plant down time significantly and make

operation more reliably and safer for the personnel. For these kinds of problems, the predictive FAC programs and calculations are good for and can reduce cost by allowing inspections to be focused on the areas where the expected corrosion rate is at highest. Or if done during the design phase, the pipe routing could be changed for a smoother radius bend to reduce the turbulence from it or even make pipe bigger to reduce the flow speed.

This is helpful information even though the actual corrosion rate might be different from the calculated one. But the benefit of adding Chromium should be percentage wise same for all the corrosion rates. When this piece of pipe is in operation and the data from the inspection is gathered for several years the actual corrosion rate can be placed over the calculated value and then calculate again the coming operating years. Similar kind of study can be for the flow speed, pipe diameter or other variable affecting the FAC rate either during design or when planning maintenance works at operating plant.

6.6   Future research topic

The future research topic for the single-phase flow calculation is the coefficients used in the commercially available tools. It is obvious from the results that this kind of coefficient is needed to create the calculation tool more precise for estimating the actual corrosion rate. It would also be beneficial to know how big of an impact the erosion-corrosion has on the corrosion rate if any. The FAC and erosion-corrosion has similar tendencies what comes to the corrosion rate and the flow speed for example. Therefore, the coefficient used in the commercially available tools might consider erosion-corrosion as one factor when calculating a wall thinning, whereas our developed tool considers only the FAC rate. Other topic would be the possibility to add the moisture content into the equation and use the same formulas for both the single- and two-phase flows. Perhaps it would be enough to use the coefficient used in the two-phase flow calculation?

For the two-phase flow calculation, the biggest disadvantage is the lack of pH factor. In the future this should be added to get more accurate data. This is extremely important for the modern pressurized water reactor plants that secondary circuits are operated at high pH levels.

Other future research topics would the parameters affecting FAC rate left out from the equations listed in chapter 4. It would be beneficial to study the impact of these parameters

and what kind of threshold values there might be for example for the oxygen content that will affect also the formation of the protective oxide layer.

7   SUMMARY

The purpose of the Thesis was to note the importance of the flow accelerated corrosion, to discuss about the potential areas and zones for the VVER that might be subject to the flow accelerated corrosion problems and to create a calculation tool to estimate the corrosion rate. The other form of corrosions was left out on purpose since those are not typically caused the operation of the plant but as failure in water chemistry and in modern NPP, the water chemistry is monitored with online monitoring systems.

The need for the thesis came from when the focus was moved to NPP operating life expectancy. Was there something that was not checked or if something should have been double checked? The most critical components were designed to last for 60 years of operation, but these were typically located in containment building and in the primary circuit. In other words, in a location where replacement was very time consuming and costly. Then the view was expanded, and the thoughts were moved towards the components and pipes of the secondary circuit. There the replacement was a lot easier because they were not nuclear safety classified and the lay-out has been designed so that the maintenance was easier.

The planned operating years was perhaps the first driving force to iniate of the thesis but soon after the first discussions, focus was moved to the maintenance and inspection plans for the unit. Idea of course was to have such a good inspection program that there were only preventive and scheduled maintenance done during operation, refueling and maintenance breaks. But since the time to do the maintenance and the inspections are limited, not all the location can be inspected as frequently. So, there should be a method of estimating what are the critical location that are inspected on a more frequent basis.

The basics of the corrosion phenomena were explained. The electrochemical corrosion or the wet corrosion is driven by the corrosion potential between the anode and cathode, both present in the metal itself. The effect of the corrosion potential between anode and cathode can be reduced by the protective oxide layer that will form on the pipe. When the protective layer is formed, the corrosion rate is dependent on the dissolution of iron oxides from it and from the base metal. This can be enhanced by the flow, that will cause the protective layer

to shrink in specific location, that will enhance the dissolution of it or iron from the base metal. This self-feeding loop is the root cause of the FAC. The other important factors listed were water chemistry, temperature, flow speed, pH and material properties of the steal.

Based on this the calculation tool for the FAC rate was developed. At the beginning of the thesis, it was clear that the calculation model is based purely on theory. First thing was to find a proper equation to start with. Therefore, the principle of the commercially available FAC software's was checked and it was decided to use the same principles. The obvious problem of not having reference data to create correction factors based on the measured or laboratory tested data came clear. All the commercially available software listed was relying on correction factors. Despite this, the models were done and the principle how they work were explained in chapter 4.

For the single phase flow the calculation had several steps. With these steps it was possible to compare the results not only by end result but also by the steps between. For the single phase flow the results where smaller than the ones in the reference article but for the Sherwood number comparison the different was not significant. Also, the fact that the difference for each location or flow parameters was not the same implies that the biggest difference to the result is done by these correction factors, otherwise the difference between equation should be equal.

The two-phase flow calculations were based on coefficient of temperature, moisture content, flow speed and Keller coefficient. From these the Keller coefficient were calculated same way in each referred document and the difference only might come from what coefficient factor for each flow restrictor had been used. Other factors were based on measured data and as we could see from the comparison the results were close to each other's. It was also calculated how the corrosion rate increases when the moisture content increases. The biggest corrosion rate was calculated on high moisture content areas as it should, but it would be beneficial to know how big of an impact the erosion corrosion has in the two-phase flows. The flow speeds are much higher in steam lines than in water lines so the probability of having erosion corrosion is higher. Also, because the moist steam contains water droplets that are known to erode pipes.

Both calculation tools worked similar way as you would expect them to, but the single-phase flow tool gives an optimistic result, and the two-phase flow gives a more conservative result. Knowing the models are not perfect does not matter since the elaborated simplified calculation models for single- and two-phase flows can still be used to make initial estimation where the FAC might occur and to choose right measures to mitigate it. For example, the material can be changed during the design or the flow speed to be reduces. The most practical example what the tools will be used is to select locations to be included into the in-service inspection program.

LIST OF REFERENCES

Baranenko, V I., Gulina O M., Naftal M M., Arefev A A., Iurmanov V A. 2013. Using of program tools for Flow accelerated corrosion estimation, VIII Intrnational Scientific and technical Conference, Safety Assurance of NPP with VVER, Podolsk, Russia, 28-31 May, 2013
Reference to original Russian version:
Бараненко В.И., Гулина О.М., Нафталь М.М., Арефьев А.А., Юрманов В.А., Использование программных средств для разчета эрозионно-коррозионного износа, 8-я международная научно-техноческая конференция Обезпечение безопастности АЭС с ВВЭР, Подольск, Россия, 28-31 мая 2013)

Delp, G. A. EPRI NP-3944 Erosion/Corrosion in Nuclear Plant Steam Piping: Causes and Inspection Program Guidelines Final Report 1985. Oley: Technicon Enterprises. 98 p.

Feron, D. 2012. Nuclear Corrosion Science and Engineering. Cambridge: Woodhead Publishing. 1072 p.

Gipon, E., Trevin, S. 2020. Flow-accelerated corrosion in nuclear power plants Nuclear corrosion: Research, progress and challenges. In Ritter, S. 2020. Nuclear corrosion: Research, progress and challenges. 472 p.

IWG-RRPC-88-1 Proceedings of a specialist meeting organized by the IAEA. In Goffin J. P. 1990. Thickness measurements of pipes submitted to erosion and corrosion problems in the steam, feed water and condensate systems of the DOEL 1 and 2 Nuclear power plants. 94 p.

McCafferty, E. 2010. Introduction to corrosion science. New York: Springer. 302 p.

NEA/CSNI/R(2014)6. Nuclear Energy Agency Topical Report. 2015. Flow Accelerated Corrosion (FAC) of Carbon Steel & Low Alloy Steel Piping in Commercial Nuclear Power Plants. 86.p.

Papavinasam, S. 2014. Corrosion control in the oil and gas industry. London: Elsevier. 918 p.

Pedeferri, P. 2018. Corrosion science and engineering. Cham: Springer International Publishing. 737 p.

Trevin, S., Moutrille M. 2012. Optimization of EDF's NPPs Maintenance due to Flow Accelerated Corrosion and BRT-CICEROTM Improvement by NDT Results Analysis. 18th World Conference on Nondestructive Testing, 16-20 April 2012, Durban, South Africa. 11p.

Typical Secondary Circuit Flow Diagram. [nuclear-power www-pages] [Referred 1.11.2021] Available at: https://www.nuclear-power.net/nuclear-power-plant/turbine-generator-power-conversion-system/from-feedwater-pumps-to-steam-generator/

Uchida, S. 2013. Determination of High-Risk Zones for Local Wall Thinning due to Flow-Accelerated Corrosion. In: E-Journal of Advanced Maintenance Vol.5-2. p. 101-112.

WANO report EAR ATL 90-017. 1990. Pipe failures in high energie systems due to erosion/corrosion Slurry 1. 22 p.

WANO report EAR TYO 04-013. 2004. Secondary pipe rupture (9 August 2004, Mihama unit 3, Kansai EPC). 17p.

WANO report WER ATL 19-005. 2019. Indian Point Unit 3 pipe wall thinning. 16p.

Calculation results for One-Phase Flow pH 9,6 and 180 °C (point 1)

Flow speed	Reynolds	Sherwood number (Sh)	FAC (for carbon steel)	in mm/s	mm in 1 year	1 year with Keller	1 year with Keller and material
1	2,39E+06	1,06E+04	1,41E-12	1,81E-13	5,70E-06	4,27E-05	1,58E-05
2	4,78E+06	1,92E+04	2,56E-12	3,28E-13	1,03E-05	7,76E-05	2,87E-05
3	7,17E+06	2,72E+04	3,63E-12	4,65E-13	1,47E-05	1,10E-04	4,07E-05
4	9,55E+06	3,48E+04	4,64E-12	5,95E-13	1,88E-05	1,41E-04	5,21E-05
5	1,19E+07	4,22E+04	5,63E-12	7,21E-13	2,27E-05	1,71E-04	6,31E-05
6	1,43E+07	4,94E+04	6,58E-12	8,44E-13	2,66E-05	2,00E-04	7,38E-05
7	1,67E+07	5,63E+04	7,51E-12	9,63E-13	3,04E-05	2,28E-04	8,43E-05
8	1,91E+07	6,32E+04	8,43E-12	1,08E-12	3,41E-05	2,56E-04	9,46E-05
9	2,15E+07	6,99E+04	9,33E-12	1,20E-12	3,77E-05	2,83E-04	1,05E-04
10	2,39E+07	7,66E+04	1,02E-11	1,31E-12	4,13E-05	3,10E-04	1,15E-04

Calculation results for One-Phase Flow pH 9,6 and 220 °C (point 2)

Flow speed	Reynolds	Sherwood number (Sh)	FAC (for carbon steel)	in mm/s	mm in 1 year	1 year with Keller	1 year with Keller and material
1	2,80E+06	1,03E+04	1,24E-12	1,59E-13	5,02E-06	3,77E-05	1,39E-05
2	5,60E+06	1,87E+04	2,25E-12	2,89E-13	9,11E-06	6,83E-05	2,53E-05
3	8,40E+06	2,65E+04	3,19E-12	4,10E-13	1,29E-05	9,69E-05	3,58E-05
4	1,12E+07	3,40E+04	4,09E-12	5,24E-13	1,65E-05	1,24E-04	4,59E-05
5	1,40E+07	4,12E+04	4,96E-12	6,35E-13	2,00E-05	1,50E-04	5,56E-05
6	1,68E+07	4,82E+04	5,80E-12	7,43E-13	2,34E-05	1,76E-04	6,50E-05
7	1,96E+07	5,50E+04	6,62E-12	8,49E-13	2,68E-05	2,01E-04	7,43E-05
8	2,24E+07	6,17E+04	7,43E-12	9,52E-13	3,00E-05	2,25E-04	8,33E-05
9	2,52E+07	6,83E+04	8,22E-12	1,05E-12	3,32E-05	2,49E-04	9,22E-05
10	2,80E+07	7,47E+04	9,00E-12	1,15E-12	3,64E-05	2,73E-04	1,01E-04

Calculation results for One-Phase Flow pH 9,6 and 150 °C (point 3)

Flow speed	Reynolds	Sherwood number (Sh)	FAC (for carbon steel)	in mm/s	mm in 1 year	1 year with Keller	1 year with Keller and material
1	2,04E+06	1,03E+04	1,53E-12	1,96E-13	6,18E-06	4,64E-05	1,72E-05
2	4,08E+06	1,87E+04	2,78E-12	3,56E-13	1,12E-05	8,42E-05	3,11E-05
3	6,12E+06	2,66E+04	3,93E-12	5,04E-13	1,59E-05	1,19E-04	4,41E-05
4	8,16E+06	3,40E+04	5,04E-12	6,46E-13	2,04E-05	1,53E-04	5,65E-05
5	1,02E+07	4,12E+04	6,10E-12	7,83E-13	2,47E-05	1,85E-04	6,85E-05
6	1,22E+07	4,82E+04	7,14E-12	9,15E-13	2,89E-05	2,17E-04	8,01E-05
7	1,43E+07	5,50E+04	8,15E-12	1,05E-12	3,30E-05	2,47E-04	9,15E-05
8	1,63E+07	6,17E+04	9,15E-12	1,17E-12	3,70E-05	2,77E-04	1,03E-04
9	1,84E+07	6,83E+04	1,01E-11	1,30E-12	4,09E-05	3,07E-04	1,14E-04
10	2,04E+07	7,48E+04	1,11E-11	1,42E-12	4,48E-05	3,36E-04	1,24E-04

Calculation results for One-Phase Flow at flow speed 6 m/s at 150 °C (pH)

pH	Iron concentration at 150 C kg/kg	Diffusivity (D) m²/s at 150 C	Reynolds number	Sherwood number (Sh)	Corrosion rate (kg/m²s)	Corrosion rate (mm/s)	Keller mm/y	(mm/y) with 1,5D elbow
7	2,5E-07	1,5E-08	1,2E+07	4,8E+04	4,5E-10	5,7E-11	1,8E-03	1,8E-02
8,7	9,3E-08	1,5E-08	1,2E+07	4,8E+04	1,7E-10	2,1E-11	6,7E-04	6,7E-03
8,9	4,4E-08	1,5E-08	1,2E+07	4,8E+04	7,8E-11	1,0E-11	3,2E-04	3,2E-03
9	3,6E-08	1,5E-08	1,2E+07	4,8E+04	6,4E-11	8,2E-12	2,6E-04	2,6E-03
9,2	2,8E-08	1,5E-08	1,2E+07	4,8E+04	5,0E-11	6,4E-12	2,0E-04	2,0E-03
9,4	8,0E-09	1,5E-08	1,2E+07	4,8E+04	1,4E-11	1,8E-12	5,8E-05	5,8E-04
9,6	4,0E-09	1,5E-08	1,2E+07	4,8E+04	7,1E-12	9,1E-13	2,9E-05	2,9E-04

Calculation for One-Phase flow at 6 m/s and pH 9,0 at different temperature

Temp. °C	Cs surface concentration of iron at pH 9	Diffusivity (D)	Schmidt number (Sc)	Sherwood number (Sh)	FAC mm/s	FAC with Keller	FAC mm/1 year with Keller
100	2,00E-08	8,50E-09	23,49	5,795E+04	2,4E-11	2,4E-10	7,7E-03
125	3,10E-08	1,25E-08	15,98	5,102E+04	4,9E-11	4,9E-10	1,5E-02
150	3,60E-08	1,50E-08	13,31	4,805E+04	6,4E-11	6,4E-10	2,0E-02
175	3,00E-08	1,80E-08	11,09	4,524E+04	6,0E-11	6,0E-10	1,9E-02
200	2,30E-08	1,95E-08	10,24	4,406E+04	4,9E-11	4,9E-10	1,5E-02
225	1,75E-08	2,50E-08	7,99	4,059E+04	4,4E-11	4,4E-10	1,4E-02
250	1,30E-08	2,90E-08	6,89	3,865E+04	3,6E-11	3,6E-10	1,1E-02
275	8,00E-09	3,40E-08	5,87	3,668E+04	2,5E-11	2,5E-10	7,8E-03
300	5,50E-09	3,85E-08	5,19	3,520E+04	1,8E-11	1,8E-10	5,8E-03

Calculation results for Two-Phase Flow at steam fraction of 0,9 and 220 °C (point 4)

Flow speed	FAC for straight pipe mm/10000h	FAC for elbow mm/10000h	FAC for elbow with 0,1% chromium mm/10000h
5	1,00E-02	7,579E-02	2,804E-02
10	2,01E-02	1,517E-01	5,613E-02
15	3,03E-02	2,276E-01	8,421E-02
20	4,04E-02	3,035E-01	1,123E-01
25	5,05E-02	3,794E-01	1,404E-01
30	6,06E-02	4,553E-01	1,684E-01
35	7,07E-02	5,312E-01	1,965E-01
40	8,09E-02	6,071E-01	2,246E-01
45	9,10E-02	6,830E-01	2,527E-01
50	1,01E-01	7,588E-01	2,808E-01
55	1,11E-01	8,347E-01	3,089E-01
60	1,21E-01	9,106E-01	3,369E-01
65	1,31E-01	9,865E-01	3,650E-01
70	1,42E-01	1,062E+00	3,931E-01
75	1,52E-01	1,138E+00	4,212E-01
80	1,62E-01	1,214E+00	4,493E-01

Calculation results for Two-Phase Flow at steam fraction of 0,85 and 180 °C (point 5)

Flow speed	FAC for straight pipe mm/10000h	FAC for elbow mm/10000h	FAC for elbow with 0,1% chromium mm/10000h
5	3,48E-02	2,613E-01	9,669E-02
10	6,96E-02	5,228E-01	1,934E-01
15	1,04E-01	7,842E-01	2,901E-01
20	1,39E-01	1,046E+00	3,869E-01
25	1,74E-01	1,307E+00	4,836E-01
30	2,09E-01	1,568E+00	5,803E-01
35	2,44E-01	1,830E+00	6,771E-01
40	2,79E-01	2,091E+00	7,738E-01
45	3,14E-01	2,353E+00	8,705E-01
50	3,48E-01	2,614E+00	9,672E-01
55	3,83E-01	2,876E+00	1,064E+00
60	4,18E-01	3,137E+00	1,161E+00
65	4,53E-01	3,398E+00	1,257E+00
70	4,88E-01	3,660E+00	1,354E+00
75	5,23E-01	3,921E+00	1,451E+00
80	5,58E-01	4,183E+00	1,548E+00

Calculation results for Two-Phase Flow at steam fraction of 0,04 and 180 °C (point 6)

Flow speed	FAC for straight pipe mm/10000h	FAC for elbow mm/10000h	FAC for elbow with 0,1% chromium mm/10000h
5	8,81E-02	6,613E-01	2,447E-01
10	1,76E-01	1,323E+00	4,894E-01
15	2,64E-01	1,984E+00	7,341E-01
20	3,53E-01	2,645E+00	9,788E-01
25	4,41E-01	3,307E+00	1,223E+00
30	5,29E-01	3,968E+00	1,468E+00
35	6,17E-01	4,629E+00	1,713E+00
40	7,05E-01	5,291E+00	1,958E+00
45	7,94E-01	5,952E+00	2,202E+00
50	8,82E-01	6,614E+00	2,447E+00
55	9,70E-01	7,275E+00	2,692E+00
60	1,06E+00	7,936E+00	2,936E+00
65	1,15E+00	8,598E+00	3,181E+00
70	1,23E+00	9,259E+00	3,426E+00
75	1,32E+00	9,920E+00	3,671E+00
80	1,41E+00	1,058E+01	3,915E+00

Calculation results for Two-Phase Flow at different steam fractions

Steam fraction	f(x)	FAC for straight pipe mm/10000h	FAC for elbow mm/10000h	FAC for elbow with 0,1% chromium mm/10000h
0,99	1,00E-01	3,59E-02	2,699E-01	9,985E-02
0,98	1,41E-01	5,08E-02	3,817E-01	1,412E-01
0,96	2,00E-01	7,19E-02	5,398E-01	1,997E-01
0,94	2,45E-01	8,81E-02	6,611E-01	2,446E-01
0,92	2,83E-01	1,02E-01	7,634E-01	2,825E-01
0,9	3,16E-01	1,14E-01	8,536E-01	3,158E-01
0,88	3,46E-01	1,25E-01	9,350E-01	3,460E-01
0,86	3,74E-01	1,35E-01	1,010E+00	3,737E-01
0,84	4,00E-01	1,44E-01	1,080E+00	3,995E-01
0,82	4,24E-01	1,53E-01	1,145E+00	4,237E-01
0,8	4,47E-01	1,61E-01	1,207E+00	4,466E-01
0,78	4,69E-01	1,69E-01	1,266E+00	4,685E-01
0,76	4,90E-01	1,76E-01	1,322E+00	4,893E-01
0,74	5,10E-01	1,83E-01	1,376E+00	5,093E-01
0,72	5,29E-01	1,90E-01	1,428E+00	5,285E-01
0,7	5,48E-01	1,97E-01	1,478E+00	5,470E-01